Effects of Temperature on Solubilization and Anaerobic Degradation of Decabromodiphenyl Ether

January 2020

Shi Chen

Effects of Temperature on Solubilization and Anaerobic Degradation of Decabromodiphenyl Ether

A Dissertation Submitted to

the Graduate School of Life and Environmental Sciences,

the University of Tsukuba

in Partial Fulfillment of the Requirements

for the Degree of Doctor of Philosophy in Environmental Studies

(Doctoral Program in Sustainable Environmental Studies)

Shi Chen

Abstract

Decabromodiphenyl ether (BDE-209), as one of the famous poly-brominated diphenyl ether (PBDE), possessed excellent physical and chemical properties due to its full-brominated structure. Therefore, BDE-209 is set as necessary anthropogenic chemicals, widely used in the textile, plastics industry, to improve the fire resistance ability of the corresponding products. Considering the contact frequency and potential toxicity of nerve inhibition, endocrine disruption, and carcinogenicity, it is of significance to degrade the BDE-209. Taking advantage of strong degradation ability in anaerobic conditions, researchers reported that BDE-209 could be degraded through reductive debromination by anaerobic microorganisms under thermophilic and mesophilic conditions. However, the difference between specific degradation characteristics in both conditions is not examined. In this research, the effects of temperature on BDE-209 anaerobic degradation are investigated. In this work, we focused on the partition, degradation rate, and pathway of PBDEs under anaerobic conditions.

Attention was paid on the partition coefficient (log K_{DOC}) for PBDE in dissolved organic carbon solution, which can help us to understand the pollutant's environmental behavior. The results for the laboratory samples, such as log K_{DOC}s for BDE-153 ether being 6.38 and 5.46 at different reaction temperatures during the cultivation procedure, suggest that a thermophilic environment may promote the solubility of PBDEs to a greater extent than mesophilic conditions. In addition, even with the same cultivate temperature, the highest log K_{DOC}s for BDE-154 are 6.71 and 6.33 in different full-scale plant digestate, illustrating the composition of DOC directly influence the PBDE solubility. Linear regression with a high R^2 of 0.9863 was also established to illustrate that the specific category of organic carbon protein, polysaccharide, lipids, and PBDE molecular structure has a direct impact on the value of log K_{DOC}. The findings from this work provided the log K_{DOC} for PBDE in anaerobic sludge DOC solution, and the equation from regression results can simulate the log K_{DOC} for PBDEs in the similar water system.

The degradation rate of PBDEs under both thermophilic and mesophilic conditions was investigated. A 200-day BDE-209 degradation experiment was carried out using a commodity curtain as a substrate. Results demonstrated that the high temperature could enhance the degradation rate of PBDEs, attributable to the high reaction activity. The overall BDE-209 degradation efficiency was not so high, less than 5% with an average mass reaction rate of 0.8 $\mu g \cdot d^{-1}$, a little bit lower than the results from previous works for five low brominated diphenyl

ethers at an initial concentration of 1 μg·mL^{-1}. Results also show that with the increase of the initial BDE-209 concentration, the degradation rate of BDE-209 rocketed, demonstrating a linear relationship between 2.5 and 10.0 mg dosing mass, at an optimal pH of 7. During the 200 days' anaerobic digestion, partial non-BDE components of the curtain may serve as a substrate, which was digested into methane and carbon dioxide with the help of active microorganisms.

Anaerobic degradation of BDE-209 was investigated in two continuously stirred tank reactors at the same time under thermophilic and mesophilic conditions for 210 days, respectively. Besides the debromination rate, the degradation kinetics of BDE-209 was also examined. The experimental results showed that thermophilic operation favored the degradation of BDE-209 in compare to mesophilic condition, achieving the maximum degradation rate of 1.1 μg·day^{-1}. The degradation mechanism of BDE-209 is associated with the replacement of bromines from polybrominated diphenyl ether with hydrogen atom, and the formation of nona-, octa- and hepta- brominated diphenyl ether gradually. In addition, its degradation well fitted the first-order kinetics. The findings from this work suggest the prospects of applying anaerobic digestion-based techniques for bromide retardant degradation.

This study offered an opportunity to realize distribution, degradation rate, and pathway of PBDEs under anaerobic conditions. These findings in this research could raise the prospects of the application of anaerobic digestion based techniques for bromide retardant degradation.

Keywords: decabromodiphenyl ether; anaerobic degradation; distribution; thermophilic condition; mesophilic condition;

Contents

List of Figures

List of Tables

Abbreviations

CSTR	continuous stirred tank reactor
DOC	dissolved organic carbon
FTIR	Fourier-transform infrared spectroscopy
GC-EI-QMS	gas chromatography/electron ionization-quadrupole mass spectrometry
hepta-BDE	heptabromodiphenyl ether
hexa-BDE	hexabromodiphenyl ether
mono-BDE	monobromodiphenyl ether
nona-BDE	nonabromodiphenyl ether
NZVI	Nano Zero-Valent Iron
OC	organic carbon
octa-BDE	octabromodiphenyl ether
PBDE	poly-brominated diphenyl ether
PCB	poly-chlorinated biphenyl
penta-BDE	pentabromodiphenyl ether
SDSAR	siphon-driven self-agitated anaerobic reactor
tetra-BDE	tetrabromodiphenyl ether
TG	thermogravimetric analysis
TOP	target organic pollutant
tri-BDE	tribromodiphenyl ether
TS	total solids
VS	volatile solids
WWTP	wastewater treatment plants
XRD	x-ray powder diffraction

Chapter 1 Introduction

1.1 Current situation of PBDE

1.1.1 Physical and chemical properties

With the continuous development and progress of society, many chemical products have entered human life. While these chemical products provide convenience and pleasure for people's lives, they also bring serious environmental pollution problems to the whole society. On the one hand, the existence of a large number of refractory pollutants has buried many hidden dangers to human health. On the other hand, the continuous emergence of pollutants has also greatly hindered the economic and cultural progress of society. Poly-brominated diphenyl ether (PBDE) is one of the most representative chemical products, researched in this study (Zhu et al., 2019).

PBDEs are widely used bromine-containing flame retardants with excellent flame retardancy through isolating flame by releasing Halogen gas on the object surface at high temperatures. They are widely used in polymers (such as high-performance polystyrene, epoxy, polyethylene, polypropylene, polyurethane sponge and nylon), paints, textiles, circuit boards, cables and wires, furniture, especially in the plastic casing of electrical and electronic products Although pentabromodiphenyl ether (penta-BDE) and octa-BDE mixtures have been banned since 2009, and the regulation of BDE-209 was mandated in 2013 by the Stockholm Convention (Roscales et al., 2018), accumulated and slow-degrading PBDEs have already built up to significant levels in the tissues of creatures exposed to environments containing this contaminant.

The chemical formula of the PBDE is $C_{12}H_xBr_yO$, and the sum of x and y is 10 ($0<=x<=9$, $1<=y<=10$). The classification of poly-diphenyl vinegar can be roughly divided into nearly ten different homologues according to the number of desert atoms. However, it is further subdivided into 209 species according to its structure and substitution sites (McGrath et al., 2017). The Table illustrates the full name and corresponding abbreviation of PBDEs involved in this paper. PBDEs and PCBs (polychlorinated biphenyls) are very similar in structure and properties, and the same primary basis is numbered and classified by the International Union of Pure and Applied Chemistry numbering system. The general characteristics of PBDEs are low vapor pressure at room temperature, strong hydrophobicity, and lipophilic characteristics.

1.1.2 Use of PBDEs in common goods

PBDEs and polybrominated biphenyls are widely produced as flame retardants and are widely used in industrial products, especially in electrical appliances, building materials, foams, upholstery, furniture, automotive interiors, etc. (Stasinakis, 2012). As the most representative PBDE of the 209 congeners, BDE-209 shows excellent physical and chemical properties due to its fully brominated structure. For this reason, market demand for BDE-209 continued to grow until the Stockholm regulation, issued in 2013 (Fang et al., 2015). Although the production and utilization of BDE-209 have been limited to a certain extent in the last few years, the cumulative amount of BDE-209 in the environment is still extremely high (Takahashi et al., 2016). Although there are 209 species of chemical PBDEs, the category of commercial PBDEs is limited. The commonly used flame retardant can be divided into three categories: Com-Penta-BDE, Com-Octa-BDE, and Com-BDE-209 (Zhang et al., 2012).

Com-Penta-BDE, a light-yellow viscous liquid, could be melted at approximate 0°C and boiled over 300°C. Com-Penta-BDE can be dissolved in hexane and has a solubility of 13 $\mu g \cdot L^{-1}$. As a mixture, is consisted of 8% tetrabromodiphenyl ether (tetra-BDE), 62% penta-BDE, a little tribromodiphenyl ether (tri-BDE), and hexabromodiphenyl ether (hexa-BDE). The majority of the composition is BDE-47 and BDE-99. The boiling temperature of it is approximate 400°C.

Different from Com-Penta-BDE, Com-Octa-BDE is a white powder. It could be melted at approximate 150°C, and the boiling temperature is approximately same as that of Com-Penta-BDE. Com-Octa-BDE can also be dissolved in hexane and has a solubility of 2 $\mu g \cdot L^{-1}$. The majority of the composition is BDE-183.

Same with Com-Octa-BDE, Com-BDE-209 is also a white powder. It could be melted at approximate 300°C and boiled into a gas over 300°C. Same with all the PBDEs, Com-BDE-209 could be dissolved in hexane. With bromide increasing, the water solubility of PBDEs decreased. Com-BDE-209 exhibits the lowest solubility, less than $0.1 \mu g \cdot L^{-1}$. Com-BDE-209 consisted of 99% BDE-209 and less than 1% nona-BDE. As the most representative PBDE among the 209 congers, BDE-209 showed excellent physical and chemical properties due to its full-brominated structure. Therefore, Com-BDE-209 is set as necessary anthropogenic chemicals, widely used in the textile, plastics industry to improve the fire resistance ability of the identical products, such as the source for polycarbonate, polyester resin, polyolefin, Acrylonitrile Butadiene Styrene, polyamide, polyvinyl chloride, and rubber. Around our daily life, in computer, TV, hairdryer, electric iron, copier, fax machine, conveyor belts, insulation

materials, rubber cables, ships and industrial materials, we found test Com-BDE-209 out. American, Euro, and Asia contributed to the 40%, 40% and 20% of the total Com-BDE-209 generation, respectively. Moreover, the marketing demand for it kept increasing until the European Union regulation issued in 2008.

1.1.3 Legal regulation

Nowadays, BDE-209 has attracted great attention worldwide and penta-BDE and octa-BDE mixtures were banned since 2009, and the regulation of deca-BDE were issued in 2013 by the Stockholm Convention (Roscales et al., 2018). And the production and utilization of DBDE has been controlled to a certain extent, the cumulative amount of DBDE in the natural environment is extremely high just due to the same reason - the excellent chemical stability. For instance, its concentration in breast milk in Taiwan had reached 1570 pg/g lipid at the end of 2017, which is three times higher than seven years previously, at 540 pg/g lipid (Chen et al., 2018b).

1.2 Toxicity

1.2.1 Neurotoxicity

For the neurotoxicity of PBDEs, it can be showed by the neurobehavior effects, disturbances in thyroid and steroid hormone homeostasis, and steroid-related effects (Darnerud et al., 2007).

The Previous study has illustrated that neonatal exposure to BDE-47 can lead to permanent aberrations in learning and memory functions for the adult animal by 3 to 10 days' mouse (Eriksson et al., 2001). Four days' contacting of BDE-47 for mice with a concentration of 100 $mg \cdot kg^{-1} \cdot d^{-1}$ decreases the concentration of circulating thyroid hormone through the nuclear receptor, CAR activating, and Mdr1a mRNA expression decreasing. Also, hepatic UGTs and transporters decreased by the circulating serum total thyroxine (Richardson et al., 2008).

Not only BDE-47 but also BDE-99 were researched. Neonatal NMRI male mice were researched with BDE-99, then the results of the radioactivity in the brain illustrated significantly impaired neural behavior presented after 3 to 10 days exposure (Eriksson et al., 2002). The levels of total circulating thyroxine were decreased after the mouse was fed with 18 $mg \cdot kg^{-1} \cdot d^{-1}$ BDE-99. Meanwhile, the neurotoxic action mechanism was different between BDE-99 and

PCB through the neurobehavioral development in the CD-1 Swiss mouse (Branchi et al., 2005).

Similar to BDE-99 and BDE-153, BDE-209 was shown to disrupt the rats' learning and memory functions by the age of 2 months through both spontaneous behavior and cholinergic system (Viberg et al., 2007). After 2 to 15 days' exposure of BDE-209 with dosing mass of 20 $mg \cdot kg^{-1}$, the ontogeny of sensorimotor responses and serum thyroxine levels in rats were analyzed, illustrated that there was a long-term behavioral change (Rice et al., 2007). Furthermore, by researching the brains from old mice, analyzed for CaMKII, GAP-43 and BDNF, the results illustrated that BDE-209 affected vital proteins, involved in healthy maturation of the brain after seven days' exposure with a BDE-209 concentration of 3 – 20.1 $mg \cdot kg^{-1}$ body (Viberg et al., 2008).

1.2.2 Endocrine disruption

The concentration of BDE-209 was researched in zebrafish embryo through the analysis of BDE-209 and its metabolic products, including octal- and nona-BDEs, with nona-BDEs being predominant. The results of triiodothyronine and thyroxine levels from the research revealed the thyroid endocrine disruption that BDE-209 influenced the levels of thyroid as well as gene transcription (Chen et al., 2012).

As the highest level animal, human beings also can be affected by PBDE. Among the obese, there were positive relationships between PBDEs and pro-inflammatory cytokines from the results of research (Zota et al., 2018). Also, PBDEs could decrease the migration distance of human neural progenitor cells through the research of disruption from thyroid hormone after a BDE-47 and BDE-99 experiment and PCR analysis (Schreiber et al., 2010). The researchers have studied not only the influence of a single person but also the transfer process in multi-generation. A total of 19 PBDEs were used to release in mother-newborn pairs.

1.2.3 Carcinogenicity

As derivatives of PCBs, PBDEs showed similar characteristics, including both in structure and chemical properties. Like PCB, the content of PBDEs in the environment is shallow. However, through the metabolism of the organism, they could be quickly accumulated in the organism and generates toxic substances. Nevertheless, at the initial stage, there is relatively little evidence that PBDEs are biologically toxic. With time going by, related studies have confirmed the biological hazard of the PBDEs, although the acute toxicity is not very high, and the skin irritation by them is also small. There has been a large number of researches on the

toxic effects of animal cells, proving that the toxicity was effect by the number of specific substituents. Also, regardless of the number of substitutions of the compound, the potential carcinogenicity effects of accumulated PBDEs (Lyu et al., 2016). Notably, the potential toxicity of historical PBDE is threatening human being all the time. For instance, the concentration of BDE-209 in breast milk in Taiwan had reached 1570 $pg \cdot g^{-1}$ lipid at the end of 2017, which is three times higher than seven years previously, at 540 $pg \cdot g^{-1}$ lipids (Chen et al., 2018b).

Researchers tested the PBDE concentration in polar bears and used a risk quotient evaluation to value its harm. The result showed that the toxic effect threshold of carcinogenicity was exceeded for all polar bear populations assessed (Dietz et al., 2015). Different from a big mammal, rats were also examined of carcinogenicity effects by PBDEs. In 2-year research, liver tumors of male and female mice were recorded, and the results exhibited that Hras and Ctnnb mutations occurred after rats' contact with PBDEs (Dunnick et al., 2018).

In order to investigate the carcinogenic risk posed to humans, Hong Kong researchers extracted PBDE and PCB from the gastric juice of human beings, who lived in an open area for e-waste depositing. The simulation results showed that with the increasing of pollutant concentration, the potential carcinogenicity increased. Moreover, the risk of PBDE is two times higher than that of PCB.

1.3 Pollution

1.3.1 Soil system

Soil experiment was also carried out in Hong Kong that typical Soxhlet extraction and multiple-step column chromatographic clean was used for soiled samples collected from an e-waste disposal site. Moreover, the results showed that less than 600 parts containing PBDE could be found in each billion soil samples (Cai & Jiang, 2006). Compared with the pure soil researching, the PBDE distribution between soil and plant tissue is much more complicated and attracted some researchers. PBDEs with low bromide atoms are easier absorbed in the roots of the plant than that with high bromide atoms. Even a linear relationship was established to simulate this distribution phenomenon (Wang et al., 2014). Also, plants harvest the PBDEs; the concentration of it in soil reduced (Huang et al., 2011). Especially after adding nitrogen fertilizer, the translocation rate of PBDEs was enhanced between soil and plants (Chen et al., 2015).

Although, China researchers contributed to most of the PBDE soil distribution research because of the severe pollution from its rapid growth of the electronics industry. However, other countries have high passionate about this research. In Turkey, a one-year investigation was

established to research eight PBDE distribution in soil, which had an average concentration of 14.45 $\mu g \cdot kg^{-1}$. Furthermore, because of its hard-degradable characteristic, BDE-209 was found as the most abundant pollutants among the eight PBDEs. Even though no significant seasonal change in the same place, the concentration increased by this order: rural, suburban, urban, industrial urban with the enhancement of industrial activities (Cetin et al., 2019). Researchers in Europeans investigated the transfer of five PBDEs between soil and air condition. Compared with soil from thick grass, the forest has a higher PBDE concentration. Lighter PBDE contributed more to the air-surface change than the heavy one. On the opposite, the heavy PBDE has a trend of deposition back to the soil after the long-distance transfer (Hassanin et al., 2004).

1.3.2 Water system

Due to the unique economic, geographical, and cultural factors, the researchers in Hong Kong focus on PBDE with a very enthusiastic passion. PBDE concentration in Hong Kong marine environment was measured. After calculating, Victoria Harbour and Sai Kung contributed the most PBDE among all the tested area. Moreover, the significant PBDEs were also BDE-47, BDE-99, BDE-153, and BDE-183, which was the same as that in the soil distribution (Liu et al., 2005). Also, six-year research was carried out in Hong Kong to reveal the PBDE pollution condition, showing that BDE-47 was the predominance pollutant in Indo-Pacific humpback dolphin tissue (Ramu et al., 2005).

Coastal water pollution is directly affected by land. The concentration of PBDEs in 25 coastal locations in Korea was determined. The results exhibited that BDE-209 was the predominant PBDE, which was consistent with the PBDE market demanding in Korea. Also, BDE-28, BDE-47, BDE-99, BDE-100, BDE-153, and BDE-154 showed a high correlated distributing condition between soil and marine (Moon et al., 2007). Later, the researcher investigated the PBDEs concentration in marine mammals from Korean coastal water. Moreover, the results revealed that the predominant PBDE is BDE-47, found in the liver and bubbler of the whales. This phenomenon is following the previous conclusion (Moon et al., 2010). Furthermore, this researching group set artificial Lake Shihwa and surrounding creeks as their target places, and the experimental results exhibited an essential relationship between organic carbon (OC) in marine and PBDE concentration in sediments (Moon et al., 2012).

1.4 Degradation methodology

1.4.1 Photo-degradation

In past decades, a considerable amount of research effort has been directed toward elucidating the degradation behavior of PBDEs (Stiborova et al., 2015a; Wang et al., 2015). Typically, the physical method, which uses ultraviolet illumination, can achieve high degradation efficiency under certain restricted experimental conditions. Bromide in the benzene ring became an activity, forming molecular remake after PBDE molecular is irradiated. Bromide atoms were abandoned from the benzene ring because of the energy change in the reaction, producing bromide ion. In this way, PBDE was debrominated into less-bromide products. So it is easy to find less-bromide diphenyl ethers in nature. However, PBDEs were hydroxylated and oxidized under the hydroxyl radicals with the illumination. In this way, accompanied by the benzene ring breaking, polybrominated dibenzo-dioxins were generated.

Researchers investigated the photo-degradation of 15 PBDEs with different bromide content in 80% methanol solution under ultra-violet light (Eriksson et al., 2004). The results showed that with an increasing number of bromine atom in PBDE molecular, the photochemical debromination rate accelerated. Different PBDEs were photo-degraded by using solid-phase micro-extraction polydimethylsiloxane fibers as photolytic support (Sanchez-Prado et al., 2005). All the results showed that the main photo-degradation product of PBDEs is the ones with losses of bromine atoms through the reductive debromination pathway.

Different from ultra-violet light, the photo-debromination of BDE-209 under irradiation with a wavelength between 300 nm and 400 nm was also researched (Ahn et al., 2006). Results revealed that shorter half-life was founded on montmorillonite or kaolinite than that on natural organic sediment. Moreover, almost no BDE-209 degradation was founded in dark circumstances. Dissolved PBDE in hexane was to carry out the sunlight photo-degradation experiments (Fang et al., 2008). All the results revealed that all the reactions followed pseudo-first-order. Also, the debromination rate decreased with a decreasing number of bromide in the PBDE substitution pattern.

BDE-209 photodegradation in both ultra-violet light and solar light were carried out together (Shih & Wang, 2009). The results showed that with the increasing of light intensity the BDE-209 degradation rate increased. Like the other experiment's results, BDE-209 photodegradation generates less-bromide products, meaning the degradation process a sequential dehalogenation mechanism. Through the formation rate of BDE-206, BDE-207,

BDE-208, the researchers indicated that the debromination position mainly occurred at para > meta > ortho.

After 30 PBDEs were exposed to sunlight for 70 h, the results released that no difference in position was found in the heavy bromide pollutants. Moreover, after benzene ring broke, poly-brominated dibenzofurans ere generated (Wei et al., 2013). BDE-209 photodegradation in an organic solvent, on silica gel, sand, sediment under ultraviolet light were focused at the same time in one work (Soderstrom et al., 2004). The results showed that different substrates almost do not influence the total photodegradation process. However, the debromination rate was strongly dependent on them. Also, PBDE was detected in the products. TiO_2 was used to photodegrade BDE-209, which can be totally removed in 180 minutes. Moreover, the degradation products include not only low-bromide PBDEs but also some oxidation products, such as bromophenol, phenols, carboxylic acid (An et al., 2008). The results suggest that during the illumination, both benzene ring and debromination occurred.

In sum, photodegradation can deal with heavy bromide pollutants, to dibromide them into less-bromide products. Nevertheless, the pure water system cannot satisfy the reaction, and the organic solvent should be added, such as methanol and tetrahydrofuran. And during the illumination, sometimes, benzene ring breaking can generate more hazard materials. So it is tough to remediate the soil and water system by pure illumination on PBDE.

1.4.2 Nano Zero Valence Iron reduction

Compared to the substrate restriction and by-product generation possibility, researchers found another way to degrade PBDEs. Taking advantage of the high reaction activity, secure handling of Nano Zero-Valent Iron (NZVI) reduction, it has become one of the most potential methodologies to deal with PBDE pollution, although this chemical reaction always generates by-products through aromatic ring destruction during degradation (Moreira Bastos et al., 2008; Shih & Tai, 2010).

To NZVI, the different microscopic scale has prominent different physical and chemical characteristics, so it does on the PBDE debromination. The results from the debromination of BDE-209 by zero-valent iron nanoparticles indicated that BDE-209 could be reduced more easily by NZVI in less than one hour than that by the Microscale Zero-Valent Iron in more than one month (Shih & Tai, 2010). The researchers also found out the acid solution is the favor for the less-bromide product, probably because that low pH is stable for the NZVI. Different from the photo-degradation, meta or ortho position is more easily to react than the para one.

Even if in the nanoscale, different ferrous reaction system showed different effects to degrade PBDE. Fe/Pd bimetallic nanoparticles were prepared, which could reduce 90% BDE-209 in 80 minutes (Zhang et al., 2015). However, the typical NZVI could just dibromide 25% BDE-209 in the same period. Because of the low affinity of the NZVI to the PBDE, Pd clusters were first adopted into the NZVI to increase its activity, then modified it with activated carbon to increase its adsorption ability (Zhuang et al., 2011). The results of the PBDEs and PCBs were more easily dehalogenation than that before, which indicated there was a hydrogen atom transfer mechanism in the new pathways. Ni/Fe bimetallic nanoparticles were synthesized with a diameter of 20 – 50 nm through chemical deposition (Fang et al., 2011a). Like the pseudo-first-order, with the increasing of Ni/Fe amount, the degradation rate increased. Also, the author predicted that hydrogen reduction is the primary debromination process.

Different from illumination, NZVI can also degrade less-bromide pollutants effectively. 6 PBDEs were used to research the effect of NZVI reduction. The researchers found that during the initial time, hexa-BDE was the most abundant products, with the progress of the reaction, tetra-BDE was the dominant product (Keum & Li, 2005). Different from some photo-degradation process, no oxidant products exist during the experiment. Like the normal dibromide phenomenon, the degradation rate decrease as the number of bromines was decreasing. Mono- and tri-BDE degradation pathways under NZVI were analyzed (Zhuang et al., 2010). However, the dibromide rate was too slow; less than 60% BDE-21 could be degraded in one month. The results indicated the degradation was a pseudo-first-order reaction and with fewer bromine substituents, the rates decreased

Despite the species of NZVI or PBDEs, the reaction system could also influence the degradation process. NZVI were used to dibromide BDE-209 in water/tetrahydrofuran solution with different volume ratio. Furthermore, the results revealed that with the increase in water content, the reaction rate had been improved. This phenomenon confirmed that the reaction was driven by the hydrogen atom (Fang et al., 2011b). The different surfactant to accelerate the rate of PBDE debromination with NZVI was investigated. The results showed a beneficial influence with a descending order: nonionic polyethylene glycol octylphenol ether > cationic cetylpyridinium chloride > anionic sodium dodecyl benzenesulfonate. Moreover, the degradation rate has a positive correlation with the surfactant concentration (Liang et al., 2014).

In sum, NZVI can primarily reduce the PBDEs in the laboratory at this time. However, in order to sustain high activity, it is hard to satisfy the reaction condition. Considering the reality of soil remediation, the application of NZVI is limited.

1.4.3 Aerobic degradation

Because of the secure handling and low cost, aerobic water treatment has been applied for several years. Moreover, the high rate of BDE-209 degradation by aerobic bacteria attracted lots of researchers' attention. Furthermore, the specific strain has been studied for a long time. Although there is enough oxygen for the bacteria to utilize, there are still two main possibilities for the products of the BDE-209 degradation, the debromination one and the hydroxylated one, or even the mineralized one. Of the different types of aerobic digestion has attracted researchers' attention in recent years (Shin et al., 2010).

Two wastewater treatment plants (WWTPs) sewage sludge in Hradec Kralove and Brno were used to degrade a mixture of PBDE, including high-bromide and less-bromide ones. After 11 months' cultivation, the total PBDE elimination reached an approximate 80%. Although the half-time of each sample is about six months, it demonstrated there was no obvious selectively in this degradation system (Stiborova et al., 2015a). Compare with the mixture, and pure 4-BDE degradation attracted researchers' attention in the aerobic atmosphere. The researcher also used toluene and diphenyl ether to stimulate the debromination. The results revealed that diphenyl ether seems to satisfy the co-metabolism better, degrading approximate 80% BDE-4 in 12 days. In the sludge, a novel species microbe *Clostridiales* was detected, which promote the BDE-4 debromination (Chen et al., 2010).

Lysinibacillus fusiformis strain DB-1, isolated from Guangdong Liangjiang River, was used to degrade BDE-209 through debromination. During the 72 h degradation, the concentration of free bromide ion increased five times from the initial 1.2 $mg \cdot L^{-1}$. The researcher also found among six category carbon source, and lactate has the best efficiency to accelerate the debromination (Deng et al., 2011). Considering the similarity between PCB and PBDE, PCB degraded bacteria, *Rhodococcus jostii* RHA1, *Burkholderia xenovorans* LB400, was used to degrade PBDEs in the anaerobic atmosphere. The results revealed that RHA completed pure debromination, however, the LB400 generated amount of hydroxylated mono-BDE (Robrock et al., 2009).

Researchers isolated the sediment from the Guangdong Guiyu e-waste dismantling area, getting bacterium, belonging to *Enterococcus casseliflavus*. Moreover, after four days' exposure, it can degrade BDE-209 80% with an initial concentration of 1 $mg \cdot L^{-1}$ (Tang et al., 2016). Also isolated from the same place in Guiyu, *Pseudomonas aeruginosa* was used to degrade BDE-209, reaching 40% in 5 days. The analysis of the seven products demonstrates the mechanism of this aerobic degradation is debromination. Furthermore, during the process,

the researcher found that a low concentration Cd ion could stimulate the reaction (Shi et al., 2013). Also, the bacteria community from the riverside with addition *Pseudomonas* sp., was used to degrade five PBDEs.

Moreover, the biologyical analysis demonstrates that 25% of core bacterial genera are standard among PBDE degraders (Yang et al., 2014). Researchers isolated a novel strain BFR01, belong to Pseudomonas sp., which could use BDE-47 as a sole source of carbon in the aerobic atmosphere, generating no lower brominated diphenyl ethers or biphenyl, and they found the optimal situation for the BFR01 is pH 7.0 and 40°C (Zhang et al., 2013). TZ-1 was found out that it had a similar character with BFR01, which could also use BDE-47 as sole carbon source, and the optimum static for it was pH 6.5 and 30°C (Xin et al., 2014). The amount of research demonstrates the PBDE degradation ability by *Pseudomonas* sp., which has attracted the researchers' attention in recent years.

A new idea has been taking out by first chemical-reduction then bio-oxidation. Korean researchers made it come true to degrade PBDEs completely. First, they used the NZVI to reduce the PBDEs, getting the low bromide products. Then, *Sphingomonas* sp. PH-07 was served to oxide the first-step products in the anaerobic atmosphere. In this way, after 20 days' reduction with NZVI concentration of 5 $g \cdot L^{-1}$ and five days' bio-oxidation, BDE-209s in the experiment were degraded (Kim et al., 2012). The joint influence between chemical and biological methods was also researched by using the anaerobic sludge in the Taiwan Erren River. After the experiment with 25 μg PBDEs in 12.5 mL serum under 30°C, the results revealed that four kinds of archaea (*Clostridium*, *Lysinibacillus*, *Rummeliibacillus*, and *Brevundimonas*) could degrade PBDEs, and the NZVI further accelerated the degradation rate (Yang et al., 2017).

1.4.4 Anaerobic degradation

Besides these methodologies above, anaerobic reduction attracted more attention because it could meet the requirement of no aromatic ring destructed byproduct generation under mild condition.

In an oxygen-free environment, with the help of a microorganism function, methane gas was generated, with the organic substrate decomposing at the same time (Mata-Alvarez et al., 2000). Anaerobic digestion has multiple advantages over the aerobic method: these include less sludge production, lower energy consumption, and energy recovery, together making it one of the most effective treatments to deal with high-strength wastewater (Shao et al., 2013). PBDE degradation under anaerobic condition was first proved by putting 10.0 nmol BDE-209s into a

100 mL serum. Sludge with primers was set as control during the 200 days experiment. The results showed that the existence of primers accelerated the debromination process rate, double as the no primers. Moreover, probably because of the hindrance, the dibromide position occurred at the meta and para regularly. Furthermore, the degradation of PBDEs that generate lower bromide products under long-term anaerobic conditions has also been investigated (Robrock et al., 2008; Song et al., 2015).

Anaerobic mixed bacteria isolated from different Taiwan river sediment were used to degrade PBDE (Yen et al., 2009). After 40 days' incubation under 30°C, the results showed that there is almost no BDE-209 degraded. Anaerobic bacteria were used to debromination the PBDE, dissolved in the trichloroethene. After two months of degradation, besides BDE-209, the majority product, other debromination products, were also generated, ranging from hexa- to mono-BDEs. A 16S rRNA gene-based analysis was carried out during the degradation, and the results revealed that *Dehalococcoides* species were present in the microorganism. The researcher also noticed that some unknown microorganism perhaps could also promote the biodegradation (Lee & He, 2010).

A study links iron cycling to anaerobic degradation of halogenated materials in natural e-waste-contaminated soil and highlights the synergistic roles of soil bacteria and ferrous/ferric ion cycling in the dehalogenation of PCBs and PBDEs (Song et al., 2015). Furthermore, Half-lives for loss of dominant PBDE congeners from sediments were decades or longer. Local agricultural soils amended with biosolids over 20 years showed a similar accumulation of PBDEs (Arnold et al., 2008).

1.5 Summary of previous researches on distribution and degradation of PBDEs

Because of high chemical stability and low bond capacity, PBDE emerged as an effective flame retardant, primarily applied in textile, plastics, electronic circuitry industry, and its market demand continued increasing (La Guardia et al., 2006). Therefore, hardly degraded PBDEs have already been multiply enriched in the creatures, exposed in the environment. Notably, the potential toxicity of historical PBDE, including nerve inhibition, endocrine disruption, and carcinogenicity, is threatening human being all the time (Lyu et al., 2016). Taking advantage of strong degradation ability in anaerobic conditions, researchers reported the BDE-209 could be degraded through reductive debromination by anaerobic microorganisms under thermophilic and mesophilic conditions. However, the difference between specific degradation

characteristics in both conditions is not examined.

1.6 Objectives of the research in this thesis

The objectives of the presented thesis are to research the distribution, degradation rate, and pathway of PBDEs under anaerobic conditions, which could be shown in Figure 1-1.

In the first research, in order to understand the partition coefficient (log K_{DOC}) for PBDE in dissolved organic carbon, 48-hour equilibrium experiment with four kinds of typical PBDE in four DOC solutions from two laboratories and two full-scale anaerobic digestion were utilized. In this way, the pollutant's environmental behavior in a similar water system would be understood, which has not been focused on before.

Secondly, attention has been given to the degradation rate of PBDEs under both thermophilic and mesophilic conditions. A 200-day activity experiment was carried out using a commodity curtain as a substrate. Meanwhile, the influence of temperature, initial substrate dosing mass, and pH was also measured. To find out the optimal degradation situation for BDE-209 debromination, especially for the temperature determination. results of all the samples were analyzed.

At last, two anaerobic continuous stirred tank reactors (CSTRs) were carried out for 210 days under thermophilic and mesophilic conditions, respectively. To compare the different degradation pathways between thermophilic and mesophilic conditions, the reaction kinetics for the multiple-step debromination reactions was investigated.

Table 1-1 The International Union of Pure and Applied Chemistry name and corresponding abbreviation of PBDE involved in this paper.

Abbreviation	International Union of Pure and Applied Chemistry name
BDE-4	4-monobromodiphenyl ether
BDE-28	2,4,4'-tribromodiphenyl ether
BDE-47	2,2',4,4'-tetrabromodiphenyl ether
BDE-99	2,2',4,4',5-pentabromodiphenyl ether
BDE-100	2,2',4,4',6-pentabromodiphenyl ether
BDE-153	2,2',4,4',5,5'-hexabromodiphenyl ether
BDE-154	2,2',4,4',5,6'-hexabromodiphenyl ether
BDE-183	2,2',3,4,4',5',6-heptabromodiphenyl ether
BDE-196	2,2',3,3',4,4',5,6'-octabromodiphenyl ether
BDE-197	2,2',3,3',4,4',6,6'-octabromodiphenyl ether
BDE-202	2,2',3,3',5,5',6,6'-octabromodiphenyl ether
BDE-206	2,2',3,3',4,4',5,5',6-nonabromodiphenyl ether
BDE-207	2,2′,3,3′,4,4′,5,6,6′-nonabromodiphenyl ether
BDE-208	2,2',3,3',4,5,5',6,6'-nonabromodiphenyl ether
BDE-209	decabromodiphenyl ether

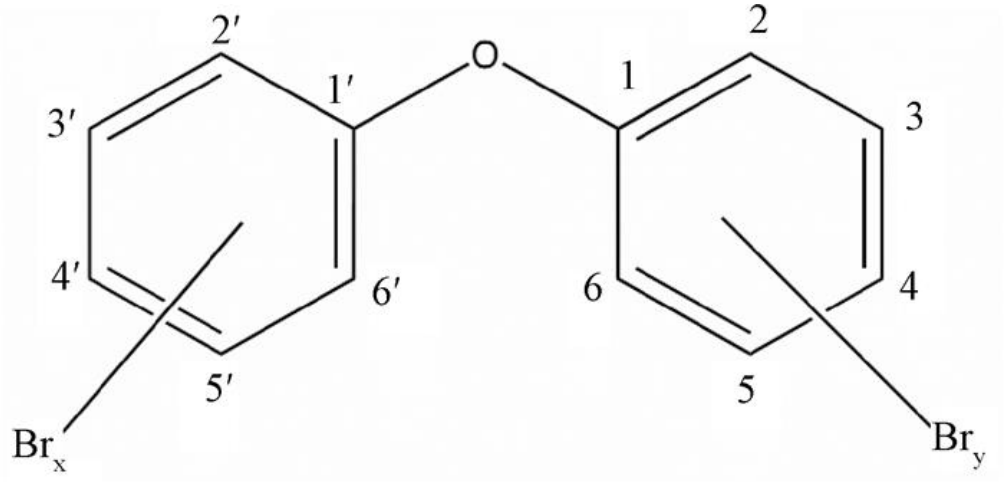

Figure 1-1 The chemical structure of PBDEs, the sum of x and y is 10 (0<=x<=9, 1<=y<=10).

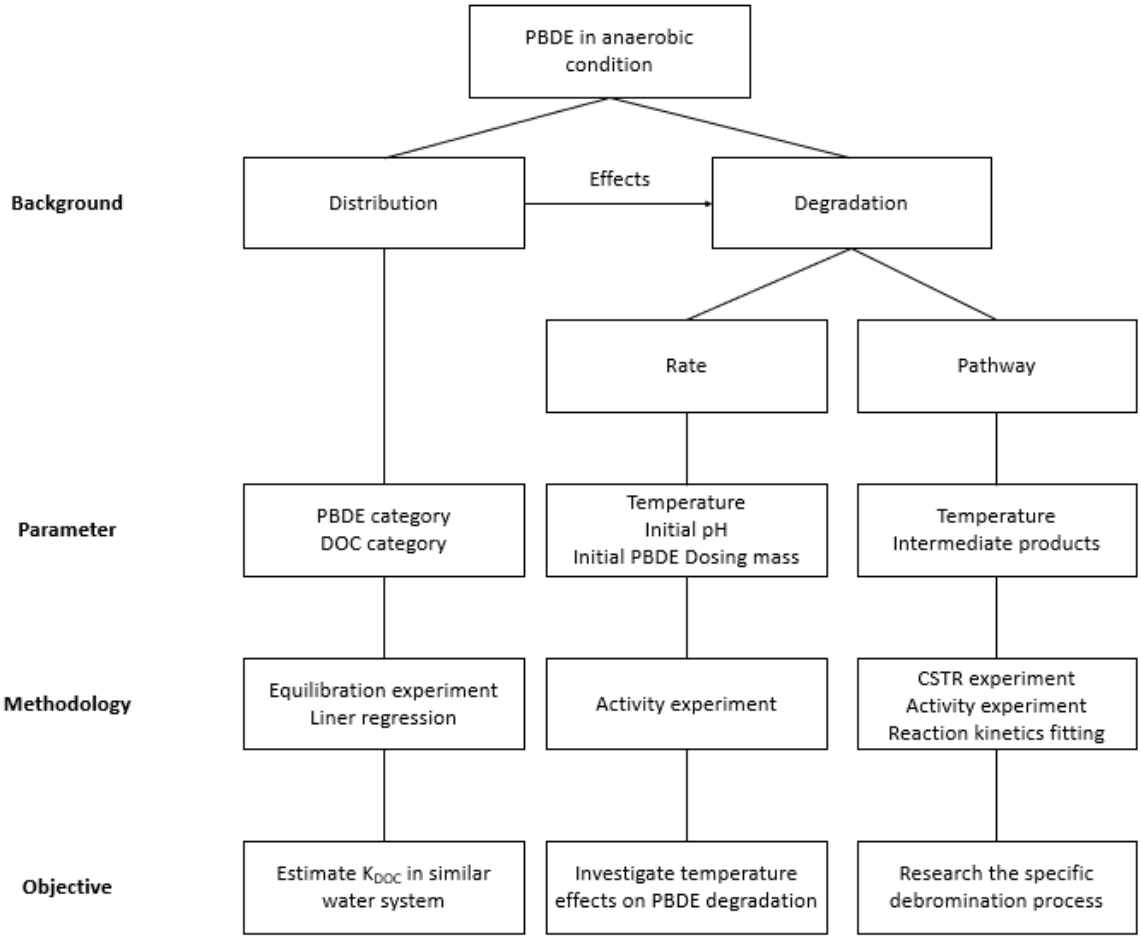

Figure 1-2 Overview of the research scheme for the three themes in this thesis.

Chapter 2 Distribution characteristics of poly-brominated diphenyl ethers between water and dissolved organic carbon from anaerobic digestate: effects of digestion conditions

2.1 Introduction

Dissolved organic carbon (DOC) can interact with target organic pollutants (TOPs) via its surface functional groups, thereby increasing the solubility of the contaminant. The positive proportional relationship between DOC concentration and the mass ratio of TOP in two phases is illustrated by Equation 2-1 below (Wei-Haas et al., 2014),

$$S_{DOC} / S_{water} = K_{DOC} \times C_{DOC} \quad (2\text{-}1)$$

where C_{DOC} is the DOC concentration in the total solution; S_{DOC} and S_{water} are the TOP concentration in the DOC and pure water phases, respectively; and K_{DOC} is the partition coefficient that leads to the DOC's solubilization effect. The coefficient for PBDE in DOC from lake water, isolated through complexation-flocculation, has been used to indicate local ecological risk (Li et al., 2015). DOC isolation methods have been compared between solid-phase micro-extraction and liquid-liquid extraction by measuring log K_{DOC} of PBDEs in sediment samples (Wang et al., 2011). Even DOC from the Arctic, isolated by solid-phase extraction, has been used to investigate the fate of PBDEs transported to polar environments (Wei-Haas et al., 2014). The log K_{DOC} values of PBDEs in simulated coastal water have also been determined to estimate the effect of the salinity of seawater on compound models (Kuivikko et al., 2010). There are also some studies on humic acid (HA) that employ log K_{DOC} (ter Laak et al., 2009). However, all studies have so far focused on natural water systems. Previous research has reported high concentrations of PBDEs in the liquid fraction of anaerobic digestate as well as the solid fraction from actual biogas plants. It is also well known that solid residues in WWTP have high PBDE concentrations (Suominen et al., 2014). Therefore, we believe that this value should be measured by liquid fractionation of samples from actual biogas plants because that high PBDE concentration in the liquid fraction is responsible for the DOC in digestate and the corresponding high log K_{DOC} value.

In this study, we focused on four typically slow-degrading pollutants: BDE-47, BDE-99, BDE-153 and BDE-154 as target organic pollutants (Parry et al., 2018), and four different filtrates from anaerobic digestion sludges formed from food waste as DOC, to carry out

equilibration experiments for the measurement of partition coefficients. In addition to the typical component analysis, Fourier-transform infrared spectroscopy (FTIR), thermogravimetric analysis (TG), x-ray powder diffraction (XRD) and zeta potential analzying were used for DOC characterization, and a linear regression was established to model the underlying log K_{DOC} in similar systems.

2.2 Materials and Methods

2.2.1 Preparation of PBDE and DOC solutions

The chemical reagents in this study, unless otherwise described, were all of analytical grade and purchased from Wako Co., Japan. Individual PBDEs (4.0 mg) (AccuStandard Inc., USA) were dissolved in 40 mL hexane to prepare 0.1 $g \cdot L^{-1}$ PBDE stock solutions. Stirring and ultrasonication were used to ensure full dissolution. All the PBDE solutions were kept in brown bottles at 4 °C until further use.

Four anaerobic sludges, originally food waste, were used as the sources of DOC for the experiment. Two laboratory sludges (Labo-T, Labo-M) were obtained from a previous study (Hu et al., 2018a), which were cultivated in a siphon-driven self-agitated anaerobic reactor (SDSAR) in a thermophilic (55 °C) and mesophilic (35 °C) environment, respectively. The other two full-scale sludges (Full-M1, Full-M2) were obtained from mesophilic anaerobic digesters treating commercial food waste, which were cultivated in a two-stage temperature-phased continuous stirred-tank reactor and in a single continuous CSTR, respectively. The sludge solution was twice centrifuged at 7,000 rcf for 20 min; the supernatant was then filtered with a 0.22-μm filter (Whatman GF/C 1822-025, GE Healthcare Life Sciences Co., USA) and the filtrate was collected as the DOC stock solution. In the equilibration experiment, COD (chemical oxygen demand) was set as the dimensional standard for measuring the DOC concentration. The solution was diluted with ultra-pure water to adjust the COD concentration of each sample to 10, 50, 100, 250, or 500 $mg \cdot L^{-1}$. For the later log K_{DOC} calculation, the unit was converted from COD into $L \cdot kg^{-1}$ OC.

2.2.2 Equilibrium experiment and log K_{DOC} calculation

A BDE-47 dosing pre-experiment was set up to confirm the suitability of the sample taking time and confirm the concentration of PBDEs in the experiment to be sufficient to carry out the later equilibration experiment. First, 0.5 mL BDE-47 hexane stock solution was added to eight

13-mL glass tubes. The tubes were then heated in a water bath at 80 °C for 10 min to evaporate the hexane, with the amount of solidified BDE-47s in the tube, approximate 200 μg, exceeding the mass of BDE-47 needed to reach equilibrium. A total of 12 mL 500 $mg \cdot L^{-1}$ Labo-M solutions was injected into the tubes. The tubes were covered with caps and shaken at 120 rpm for 96 h in an incubator at 35 °C. During the equilibration process, 24, 48, 72 and 96 h were set as the dwelling times, as in previous research (Wei-Haas et al., 2014).

In the formal equilibration experiment, the specific experimental scheme was the same as in the pre-experiment. The categories and concentrations of PBDE and DOC solutions matched the experimental conditions. Three duplicate samples were set up for each condition. The equilibration reaction time of 72 hours was selected in the light of the results of the pre-experiment.

As it is very difficult to measure the concentrations of PBDEs in DOC alone, the PBDEs from the whole solution were extracted and analyzed. Based on Equation (2-1), Equations (2-2) and (2-3) are established as follows,

$$S_{solution} / S_{water} = K_{DOC} \times C_{DOC} + 1 \quad (2\text{-}2)$$

$$S_{solution} = S_{DOC} + S_{water} \quad (2\text{-}3)$$

with $S_{solution}$ being the concentration of PBDE in the whole solution. This allowed the partition coefficient to be calculated directly from the measured value of $S_{solution}$, S_{water} and C_{DOC}. A linear relationship between $S_{solution}/S_{water}$ and DOC concentration was established, and further fitted with the R^2 and P-values.

2.2.3 Sample preparation and analysis

The supernatant of each sample was filtered via a 0.22-μm filter to remove any excess PBDE after the equilibration experiment. PBDEs were extracted from the filtered solution twice: first to remove the high quantity of DOC, and then to remove any trace organic matter. After the addition of 10 mL of filtering solution to the separating funnel, the PBDEs in the solution were extracted three times with 15 mL dichloromethane. The extraction solution was harvested with a final volume of approximately 45 mL in 50 mL tubes. After the dichloromethane had been evaporated at room temperature in a fume hood, 3 mL hexane was utilized to dissolve the small amount of PBDE. The mixture solution was diluted with a small volume of hexane to bring it to a constant volume of 10 mL and placed in the dark for further extraction. Further, for the experiment to select sample taking time, all the PBDEs in the experiment, including those on the filter paper and inner walls of tubes, were extracted and dissolved in the same way as

described above.

The purification of PBDE was followed the practice of a previous study (Matsukami et al., 2017). 1 mL extracted PBDEs solution was added into the column, filled with the following component from bottom to top: 0.3 g DX gel, 3 g 2% KOH silica, 0.3 g DX gel, 4.5 g 44% H_2SO_4 silica, 6 g 22% H_2SO_4 silica, 0.3 g DX gel, 1g Na_2SO_4, with 70 mL 5% dichloromethane in hexane (DCM/HEX) as the mobile phase. Then an active carbon-dispersed silica gel reversible column, $^{13}C_{12}$ (Cat 01894-96, Kanto Chemical Co. Inc., Japan) with 80 mL 25% DCM/HEX solution as the mobile phase.

The extracted and prepared PBDE content in hexane concentration was measured using a gas chromatography/electron ionization-quadrupole mass spectrometry (GC-EI-QMS) system (5975C GC/MSD system, Agilent Technologies Inc., USA) equipped with a 15 m × 0.25 mm × 0.1 μm capillary column (DB-5MS, Agilent Technologies Inc., USA). In reference to the laboratory quality assurance and quality control procedures, an Ultraviolet-off mode was applied in the sample measurement to prevent PBDEs degradation. A set of calibration solution mixtures were prepared for BDE-47 and BDE- 99 (0.5-200 $ng \cdot mL^{-1}$), BDE-153 and BDE-154 (1-400 $ng \cdot mL^{-1}$), reflecting a good linearity ($R > 0.99$) of calibration curve by GC–EI-QMS measurement. The recoveries of internal standards were found to be 78% for BDE-47, 85% for BDE-99, 80% for BDE-153, 88% for BDE-154, respectively. The detection limits for all samples were in the ranges of 0.02-0.09 $ng \cdot g^{-1}$ for PBDE congeners.

2.2.4 Sludge and DOC analysis

Total solids (TS), volatile solids (VS), OC, protein, polysaccharides, lipids and COD were analyzed according to the US EPA Standard Method. A microscope (Eclipse E1000, Nikon Co., Japan) was used to observe the PBDEs suspended in ultra-pure water to identify the particle size of undissolved PBDEs for the selection of a filter paper with a suitable pore size.

To preserve the organic structure of DOC, we evaporated the water from the DOC solution at room temperature to obtain a dry precipitate. This precipitate was then ground into a powder for further morphology characterization. The functional groups of the DOC were identified using an FTIR spectrometer (Nicolet iS5, Thermo Fisher Scientific Inc., USA) within the wavenumbers of 400 cm^{-1} to 4000 cm^{-1}. Thermogravimetric variation was measured under a nitrogen atmosphere between 20 °C and 500 °C using a Thermo plus EVO2 (Rigaku Co., Japan).

2.2.5 Linear regression establishment

After unit conversion into OC, we set proteins, polysaccharides and lipids as independent parameters for DOC composition. Meanwhile, considering the molecular steric configuration of PBDE, we set the value of the fitting coefficient at 1 to indicate that there are bromine atoms on the corresponding position of PBDE and set it at 0 if there were no bromine atoms in the given position. Nevertheless, due to the limited number of PBDE samples in this study, we focused on only three bromine atom positions (5, 5', and 6') around two benzene rings. All the independent parameters were used to carry out the linear regression fitting using mathematical statistical software (SPSS Statistics 22, IBM Co., USA), illustrated by Equation 2-4 as follows,

$$\log K_{DOC} = K_1 \times \text{protein content} + K_2 \times \text{polysaccharide content} + K_3 \times \text{lipid content} + K_4 \times 5 \text{ position} + K_5 \times 5' \text{ position} + K_6 \times 6' \text{ position} + B \quad (2\text{-}4)$$

where K_1, K_2, and K_3 are the fitting coefficients for the concentrations of protein, polysaccharides and lipids, respectively; K_4, K_5, and K_6 are fitting coefficients for the presence or absence of a 5, 5' and 6' position bromine atom, respectively; and B is the intercept.

2.3 Results and Discussion

2.3.1 Characteristics of DOC and equilibration experiment preparation

The basic characteristics of initial sludge and prepared DOC are presented in Table 2-1. Except the Full-M2 sample, the water content for these 3 samples is relatively high, reaching 99%. The amount of VS for two laboratories and Full-M2 sludge is approximately half of the TS, apparently higher than that of the Full-M1 one. The diversity of composition of original sludge from different cultivate environment provides multifarious DOC in this research.

Figure 2-2 (a) illustrates the FTIR spectrum of the sample powder, which were evaporated and milled from the DOC solution. It is obvious to see that the FTIR spectrum of the Labo-T, Full-M1 and Full-M2 samples are similar, totally different from that of Labo-M. Specifically, the sharpest peak at 1,450 cm^{-1} of these three samples could be regarded as the symmetrical stretching of carboxyl (Smidt et al., 2011). And the existence of methyl and methylene in Labo-M sample is proven by the small peaks at 1,400 cm^{-1} and 1,450 cm^{-1}, respectively. Meanwhile, the continuous multi-peak around 1650 cm^{-1} in each line is attributed to the same function group-aromatic ring, which is in agree with the previous researches (Chin et al., 1997; Chiou et al., 1998). The spectrum for Labo-M and Full-M2 sample have the wide broad peak with a wavenumber between 2,750 cm^{-1} and 3,250 cm^{-1}, caused by the H-O stretching vibration due

to the existence of hydroxyl in the DOC composition and the tiny amounts of adsorbed water from room air. However, the other two samples of the Labo-T and Full-M1 have three peaks at 2,780 cm^{-1}, 3,040 cm^{-1} and 3,115 cm^{-1}, which were considered to belong to the typical =C–H and –C–H stretching vibration. There is also meticulous distinction among the whole four samples. The little peak around 1080 cm^{-1} indicated the probable presence of stretching of the P–O, N-O from protein. However, the obvious peak at 1,010 cm^{-1} in the other two samples showed the strong –C=O stretching (Zhang et al., 2016). The characteristic peak at 880 cm^{-1} from the Full-M2 sample spectrum illustrated the potential C=C skeleton among the DOC composition. From the FTIR spectrum, it can be seen that the four samples shared some common functional groups on one side but featured with some particular ones, revealing that the composition of them differs from each other. Nevertheless, it is difficult to get any quantitive information about the content of every functional groups based on the rare FTIR spectra.

Figure 2-2 (b) shows that the TG plots of four DOC solid samples were divided into several weight loss zone indicating the decomposition of different compositions with temperature rising from 25°C to 500°C. The water volatilization between 30°C and 150°C accounted for approximate 30% and 15% of the weight loss for Labo-M and Full-M2 sample, while there is almost no weight loss for Labo-T and Full-M1 in this temperature range, reflecting the difference of water content in these four samples and is in consistence with the analysis by FTIR graphs (Smidt et al., 2011). Especially, two steps of water evaporation and small molecular containing carbonyl reduction were proposed for the Labo-M sample. When temperature is higher than 150°C, the Labo-T, Full-M1 and Full-M2 samples showed almost the same weight loss tendency. The Full-M1 sample showed one sharp decreasing between 200°C and 250°C, which indicates the decomposition of carboxylic groups and corresponds to the 1450 cm^{-1} peak of FTIR spectrum. However, the Labo-T and Full-M2 samples illustrated another zone of weight loss between 250°C and 350°C and is assumed to be due to the oxidation of carbon-containing molecules such as lipid (Miyazawa et al., 2000), which is also in consistence with the lipid content tendency illustrated in Table 2-1. Between 400°C and 500°C, there are only small amount tailings left. Because of the low temperature and the possibility of carbonize chalking from protein, polysaccharide or any other organic matters, the weight loss of total sample is approximate 50% (Idris et al., 2010).

Electrical double-layer on the DOC particle surface is illustrated by zeta potential through the protonation and deprotonation functional group (Yuan et al., 2011). Zeta potential was carried out by making a suspension solution of DOC particles in deionized water. The DOC

solution was made homogeneous through supersonic treatment for 30 min before analysis. With pH increasing, higher OH- concentration of in solution will result in more hydroxide groups accumulating on the DOC particle, thus the surface charge of DOC molecules was observed to be negative and the zeta potential of the DOC solution decreased (Figure 2-2 (d)) (Patil et al., 2007). It should be noted that the zeta potential for Labo-M with less-negative surface charges is higher than the other three samples at pH of 7, and this can be related to the existence of carboxyl group on this sample verified by FTIR results. The four samples have a high variety concerning the functional groups, organic matter composition and surface charging situation, making a good guarantee for obtaining different log K_{DOC} value of these four samples, which is important for the discussion of log K_{DOC} in the following parts.

2.3.2 Log K_{DOC} for PBDEs between water and DOC

Figure 2-4 clearly shows a linear relationship between $S_{solution}/S_{water}$ and COD concentration. Presumably, $S_{solution}/S_{water}$ is higher than 10 owing to the outstanding solubility of PBDEs, which appears greater than that suggested in previous research (Wei-Haas et al., 2014). Because of solubility differences and errors in measurements, the standard error for a single value of a low-bromine PBDE is lower than that of a higher-bromine BDE. For all the 16 fitting results for the linear relationship in Table 2-2, except for three measurements (BDE-99 in Lab M, BDE-153 in Lab M and BDE-153 in Full M2) that show less linearity with R^2 values below 0.81, the others all show a good linear relationship between $S_{solution}/S_{water}$ and COD concentration, with a value of R^2 greater than 0.90. Four experimental results (BDE-153 in Lab T, BDE-154 in Lab T, BDE-47 in Lab M, BDE-153 in Lab M1) showed a particularly clear linear relationship, with P-values of less than 0.0001. However, for BDE-153 in the Lab M and Full M2 samples, the linearity of the $S_{solution}/S_{water}$-COD concentration curve declined in the high COD concentration range, with a lower observed $S_{solution}/S_{water}$ value than predicted by our linear model. This may be due to the extremely high DOC concentration causing dissolved organic matter to clump together, resulting in fewer active sites being available to react with PBDEs. In a similar study on PCBs, the same rationale was used to explain the phenomenon of log K_{DOC} decreasing with increasing DOC concentration (Chin et al., 1997).

Experimental log K_{DOC}, measured in $L \cdot kg^{-1}$ OC, is calculated from the linear slope and OC, converted from the measured COD. Their corresponding comparisons are shown in Figure 2-5. The average of log K_{DOC} for Lab T, Full M1, and Full M2 sample is approximately 6.3, higher than that for Lab M, which is 5.3, which is also in agreement with the similar trend seen in the

FTIR analysis. The comparison of log K_{DOC} between the Lab T and Lab M samples shows that temperature plays an important role in influencing the variety of DOC in sludge. This is supported by the fact that even though the sludge was digested in reactors of the same design and fed with the same substrate, thermophilic or mesophilic conditions led to completely different DOC categories. The presence of small molecules from the decomposition of amino acids and sugars could be one reason for the log K_{DOC} for Lab M being the lowest: this is consistent with the TG plots. However, DOC obtained under different digestion temperatures could possess similar solubilization properties among the Lab T, Full M1 and Full M2 samples. To conclude, the category of DOC directly affects its specific composition, which includes molecular weight, presence of aromatics, wide contrasts in polarity, etc. (Akkanen et al., 2004).

Table 2-2 and Table 2-3 show a comparison of log K_{DOC} for BDE-47, BDE-99, BDE-153 and BDE-154 in DOC solutions from different studies. It can be seen that when the number of bromine atoms increases from 4 to 6, log K_{DOC} also increases as more active sites (Br atoms) for DOC combination became available. This result is in accordance with the relationship between log K_{DOC} and the numbers of chlorine atoms in PCBs (Durjava et al., 2007). The divergence value of log K_{DOC} between tetra-BDE and hexa-BDE in the results of most other studies is 1.0, higher than the value of approximately 0.4 obtained for our samples. For tetra-BDE and penta-BDE, the log K_{DOC} values for the Lab T, Full M1 and Full M2 samples are similar to those for DOC in simulated coastal water (Kuivikko et al., 2010), and higher than those for the Lab M sample. The log K_{DOC} of the sediment sample from the Arctic is generally lower than that for the other samples, including those from the Suwannee River, typically with FA (fulvic acids) with high levels of aromaticity; thus the authors pointed out that not only aromaticity alone, but also polarity and molecular weight, may affect the already complex reactions (Wei-Haas et al., 2014). Another previous study has revealed that the affinity of PBDE combinations with HA is higher than that with FA (DePaolis & Kukkonen, 1997). However, the log K_{DOC} values for the Lab T, Full M1 and Full M2 samples are even higher than those for Leonardite, a typical HA (Zhao & Qiao, 2010), which means that neither HA nor FA is likely to be the main component of these three samples: this is consistent with the residual/total COD analysis (Table 1). Even for the Lab M sample, no more than 4% of the total sample is likely to be HA or FA. The log K_{DOC} for our hexa-BDE sample is similar to that of previous results (Wang et al., 2011), but the results for tetra-BDE and penta-BDE are dramatically different from ours. In almost all cases, the log K_{DOC} of BDE-154 is lower than that of BDE-153 in the Labo-T, Lab o-M and Full-M2 samples, which is consistent with previous research on PCBs. Because

the ortho-substituted bromine atom hinders PBDE molecular rotation through the oxygen atom, the probability of combination between DOC and PBDE decreases with smaller log K_{DOC} values (Uhle et al., 1999). Above all, the log K_{DOC} values for our samples are higher than the overall level of that for natural water or sediment containing HA or FA, etc. (ter Laak et al., 2009). Instead, most DOC from anaerobic digestion consists of proteins, polysaccharides, lipids, and similar substances.

Accurate measurement of S_{water} guarantees the calculation of K_{DOC}, with the former being used as the denominator. The K_{OW} of a contaminant can be used to model its distribution between water and organic phases and to predict its fate or persistence during movement, illustrated as follows in Equation 2-5,

$$K_{ow} = S_{octanol} / S_{water} \quad (2\text{-}5)$$

where $S_{octanol}$ and S_{water} are the contaminant's solubility in octanol and water respectively. Because of their similar physicochemical behavior during distribution, there is a linearity between log K_{OW} and log K_{DOC} (Cho et al., 2002). Figure 2-6 is a scattergram created using log K_{DOC} values from our samples. Log K_{OW} (Katsoyiannis & Samara, 2006). The relatively good linear relationship also demonstrates the accuracy of the calculation for log K_{DOC}.

2.3.3 Simulation of log K_{DOC} by linear regression

The methodology of linear free energy relationships is a well-established technique for calculating the equilibrium partition coefficients in multiple systems and for estimating K_{DOC} for PBDEs (Stenzel et al., 2013; Wei-Haas et al., 2014). However, no research has yet been carried out to directly correlate the relationship between the components of a solution and log K_{DOC}, especially typical organic substances such as polysaccharides and lipids.

Almost all ranges between fitting and measurement are less than 0.12 with a R^2 of 0.96, suggesting very good fitting results. K_1 showed the smallest value, owing to a high protein content and a possibly weak correlation with K_{DOC}. Figure 2-7 also supports our hypothesis through a high R^2 of 0.9766 from a linear fitting between the estimated value and log K_{DOC} derived from the experimental measurements. Because the number of samples of PBDEs in our study is the same, the three coefficients for bromine atom position (K_4, K_5, and K_6) showed similar errors. This suggests the feasibility of our linear regression method for estimating partition coefficients based on the components of the solution and the positions of the bromine atoms. However, the split amount and degree of congruence in this database are relatively small due to the characteristics of the PBDE samples.

2.4 Summary

After 48-hour equilibrium experiment, the laboratory samples' results exhibit that the log K_{DOC} of Lab T is higher than that of Lab M, which indicates that thermophilic sludge favors the solubilization of PBDEs. A comparison of Lab M, Full M1, and Full M2 samples revealed that even at the same digestion temperatures, different DOC categories can lead to different solubilization properties. The value of log K_{DOC} can be simulated through a linear regression that combines the impact between the specific category of organic carbon and the PBDE molecular structure.

Table 2-1 Digestion environment and main basic parameters measured for the sludge and DOC solutions used in this study (means of triplicate measurements).

Category	Parameter	Labo-T	Labo-M	Full-M1	Full-M2
Source sludge	Reactor design	SDSAR	SDSAR	CSTR	CSTR
	TS ($g \cdot L^{-1}$)	1.56 ± 0.17	5.04 ± 0.23	3.00 ± 0.04	26.23 ± 1.89
	VS ($g \cdot L^{-1}$)	0.71 ± 0.07	3.07 ± 0.31	0.13 ± 0.03	17.02 ± 0.12
DOC solution	OC ($mg \cdot L^{-1}$)	528 ± 88	272 ± 56	424 ± 104	1092 ± 128
	Proteins ($mg \cdot L^{-1}$)	235 ± 28	155 ± 15	616 ± 118	729 ± 130
	Polysaccharides ($mg \cdot L^{-1}$)	72 ± 1	15 ± 12	111 ± 24	318 ± 16
	Lipids ($mg \cdot L^{-1}$)	276 ± 55	143 ± 34	130 ± 22	213 ± 49
	Total COD ($mg \cdot L^{-1}$)	1341 ± 206	676 ± 101	1722 ± 200	2359 ± 103
	Residual / Total COD *	9.55%	3.14%	17.72%	13.36%

* Calculated Residual / Total COD Ratio

= (Total COD – 1.51 × Proteins – 1.07 × Polysaccharides – 2.83 × Lipids) / Total COD × 100%

Table 2-2 Comparison of log K_{DOC} for the different environments and temperatures in this study.

DOC Source	Temp.(°C)	BDE-47	BDE-99	BDE-153	BDE-154
Labo-T	35	5.93 ± 0.03	6.02 ± 0.07	6.38 ± 0.03	6.33 ± 0.03
Labo-M	35	5.05 ± 0.02	5.21 ± 0.11	5.46 ± 0.12	5.35 ± 0.05
Full-M1	35	6.18 ± 0.05	6.67 ± 0.06	6.62 ± 0.03	6.71 ± 0.05
Full- M2	35	6.10 ± 0.03	6.45 ± 0.06	6.45 ± 0.12	6.33 ± 0.06

Table 2-3 Comparison of log K_{DOC} for the different environments and temperatures of previous study.

DOC Source	Temp. (°C)	BDE-47	BDE-99	BDE-153	BDE-154	References
Toolik Lake (Arctic)	23	4.17 ± 0.12	4.70 ± 0.12	5.07 ± 0.15	-	Wei-Haas et al., 2014
Imnv Creek (Arctic)	23	4.29 ± 0.12	4.71 ± 0.16	-	-	Wei-Haas et al., 2014
Sagavanirktok (Arctic)	23	4.04 ± 0.13	4.47 ± 0.20	5.00 ± 0.15	-	Wei-Haas et al., 2014
Suwannee River (US)	23	4.70 ± 0.10	5.12 ± 0.05	5.16 ± 0.10		Wei-Haas et al., 2014
Lake humic acid	25	5.11 ± 0.06	5.41 ± 0.06	5.64 ± 0.16	5.65 ± 0.07	Li et al., 2015
Jordan Lake (US)	-	6.19 ± 0.11	6.31 ± 0.02	7.20 ± 0.04	7.10 ± 0.05	Wang et al., 2011
Greasy Creek (US)	-	5.48 ± 0.02	6.10 ± 0.02	6.43 ± 0.22	6.35 ± 0.17	Wang et al., 2011
Leaf Lake (US)	-	5.48 ± 0.01	5.58 ± 0.01	7.24 ± 0.22	7.20 ± 0.05	Wang et al., 2011
San Diego Creek (US)	-	5.81 ± 0.03	6.30 ± 0.03	7.13 ± 0.04	7.18 ± 0.01	Wang et al., 2011
River Mustio, Finland	20	6.65 ± 0.04	6.52 ± 0.00	-	-	Kuivikko et al., 2010
Tammisaari, Finland	20	6.56 ± 0.07	6.82 ± 0.02	-	-	Kuivikko et al., 2010
Hermanso, Finland	20	6.46 ± 0.05	6.53 ± 0.02	-	-	Kuivikko et al., 2010
Vastergadden, Finland	20	6.40 ± 0.04	6.33 ± 0.00	-	-	Kuivikko et al., 2010
Humic Acid Sodium Salt	20	5.97 ± 0.06	6.37 ± 0.06	6.73 ± 0.07	-	ter Laak et al., 2009
Leonardite	25	5.80 ± 0.05	5.97 ± 0.02	5.39 ± 0.02	5.48 ± 0.02	Zhao & Qiao, 2010

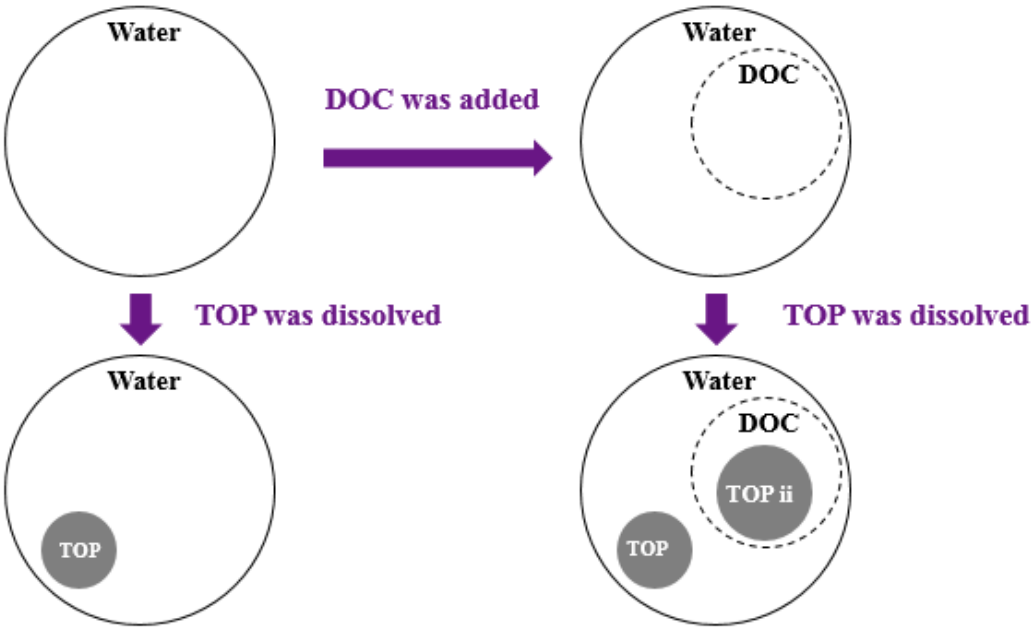

Figure 2-1 The solubilization effect of target organic pollutant (TOP) by adding DOC (TOP ii is solubilized TOP content after DOC added).

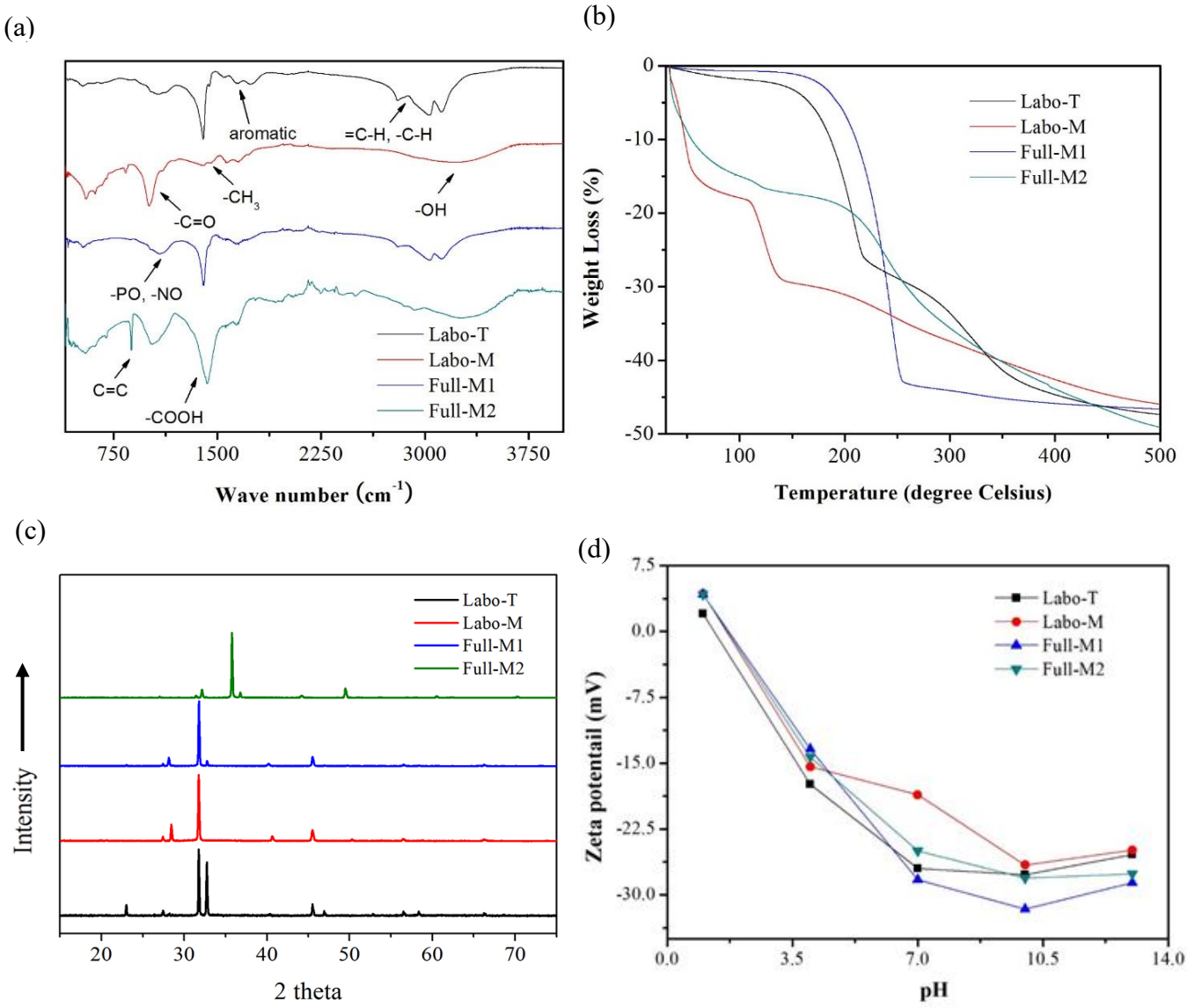

Figure 2-2 (a) FTIR graph with the wave number between 500 and 4000 cm^{-1} for four DOC solid samples; (b) TG graph of four DOC solid samples with heating temperature from 30 to 500°C under nitrogen atmosphere; (c) XRD patterns of four DOC solid samples; (d) Zeta potential for four DOC solutions with COD concentration of 500 $mg \cdot L^{-1}$ at pH 1, 4, 7, 10, 13.

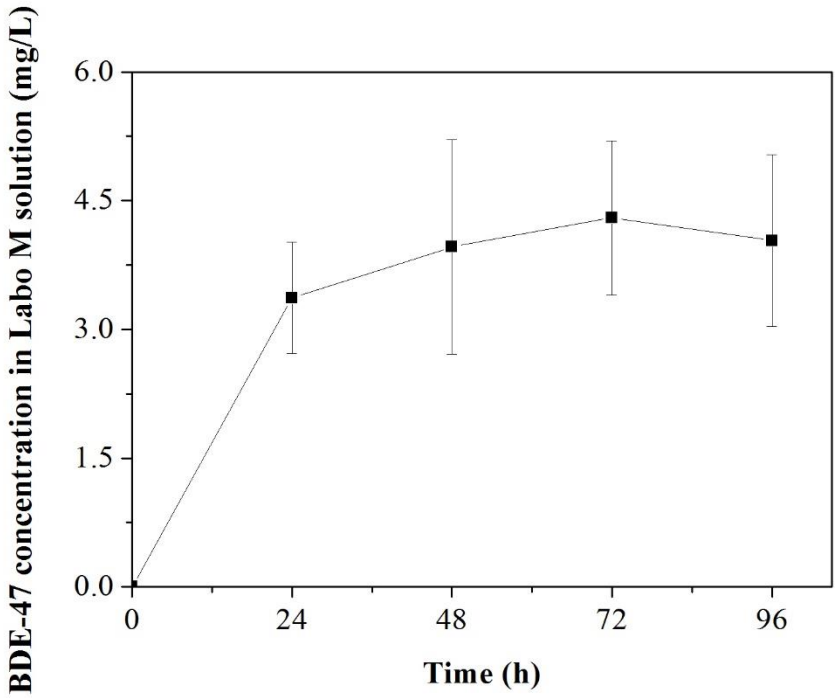

Figure 2-3 BDE-47 concentration change in 500 mg$\cdot$L^{-1} Labo-M solution during 96 hours of the equilibration experiment preparation.

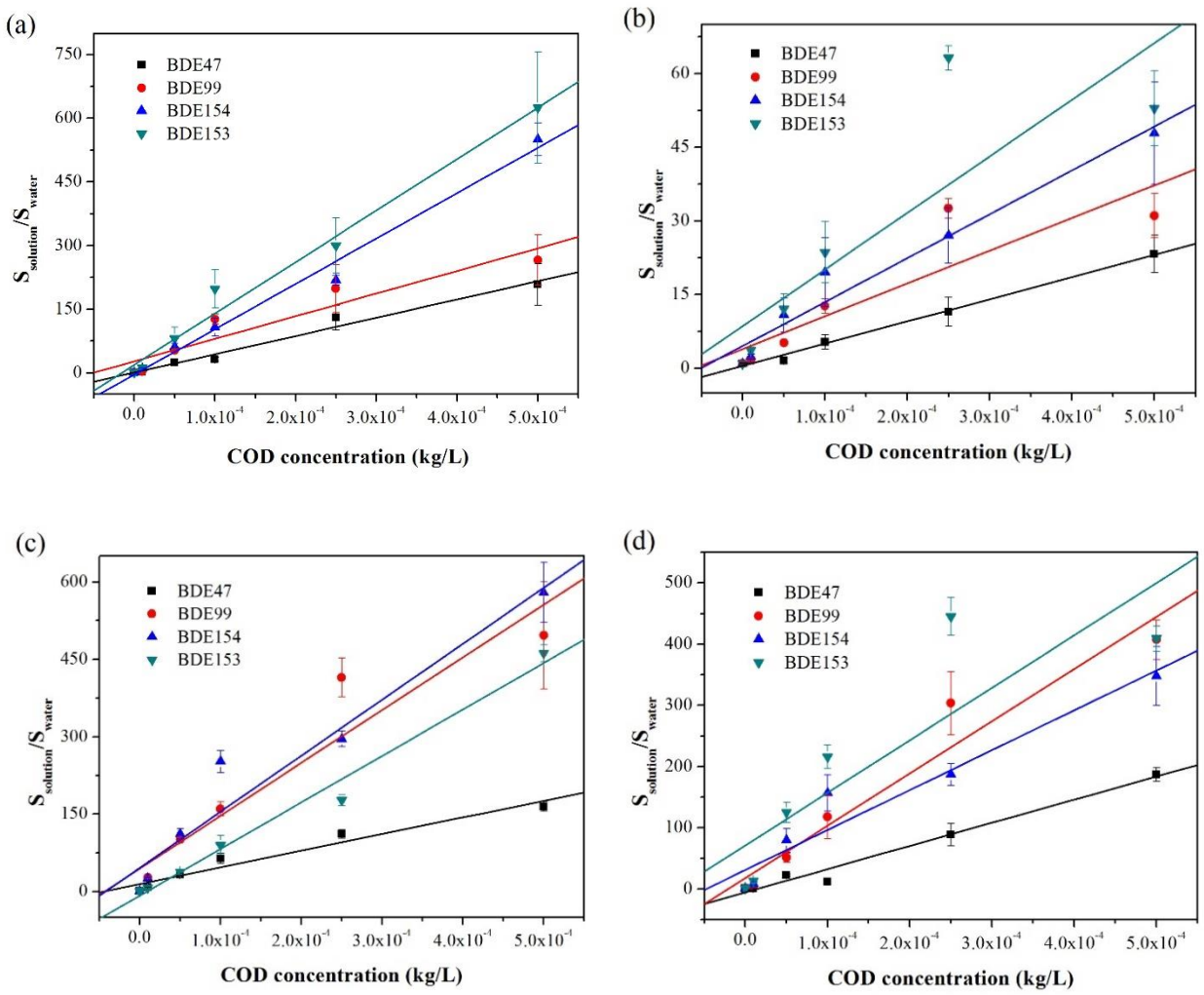

Figure 2-4 Fitting linear relationship between the $S_{solution}/S_{water}$ and COD concentration of four DOC categories and PBDEs: (a) Labo-T; (b) Labo-M; (c) Full-M1; (d) Full-M2.

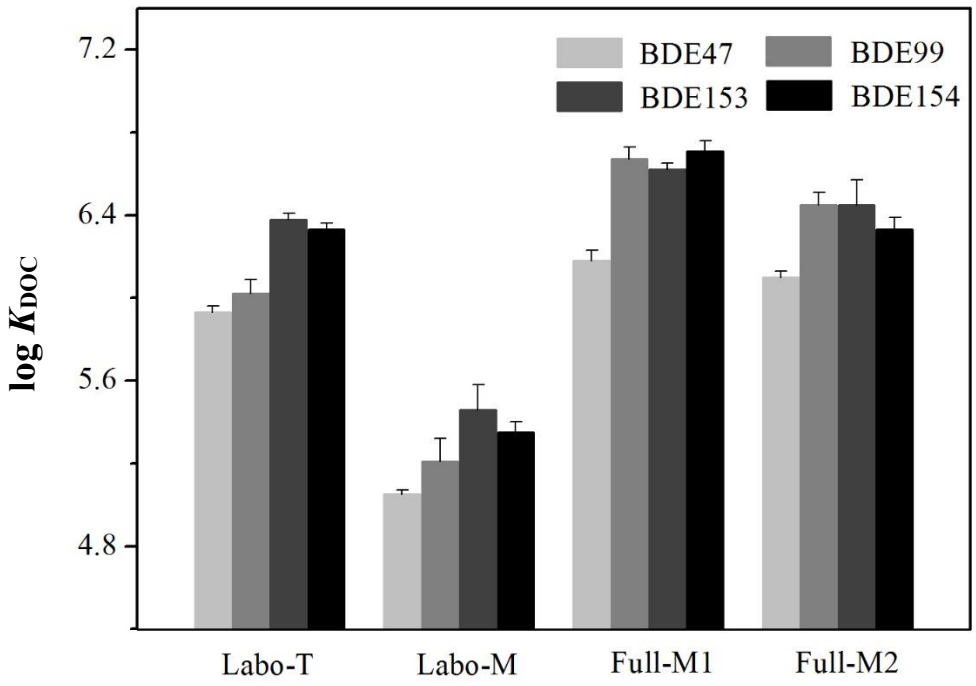

Figure 2-5 Summary of measured log K_{DOC} values for PBDE congeners using four DOC solution. Labo-T and Labo-M are the two laboratory sludges. And Full-M1 and Full-M2 are the two full-scale reactor sludges, specifically.

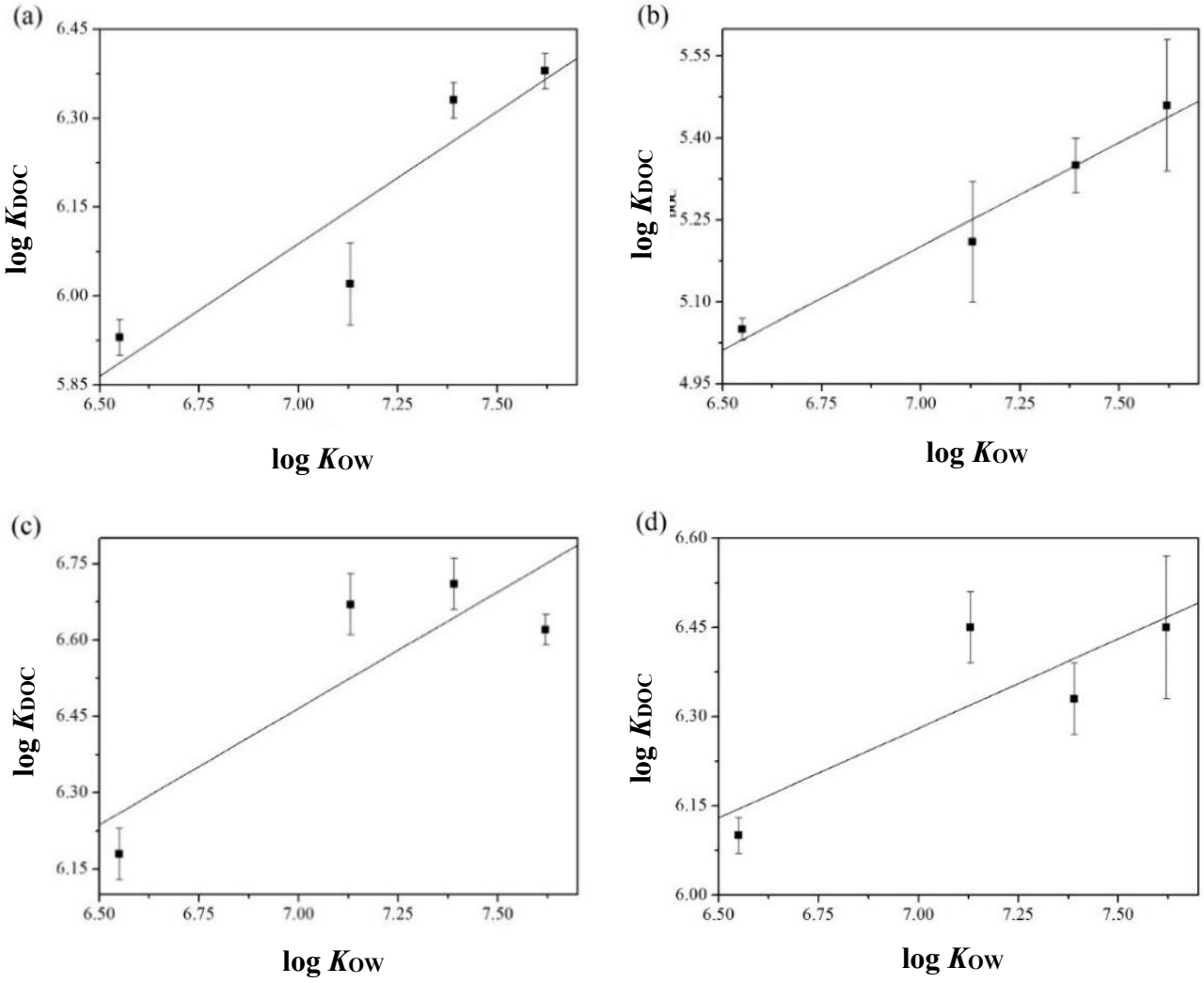

Figure 2-6 Fitting linear relationship between the log K_{DOC} and log K_{OW} for 4 DOC categories: (a) Labo-T; (b) Labo-M; (c) Full -M1; (d) Full-M2.

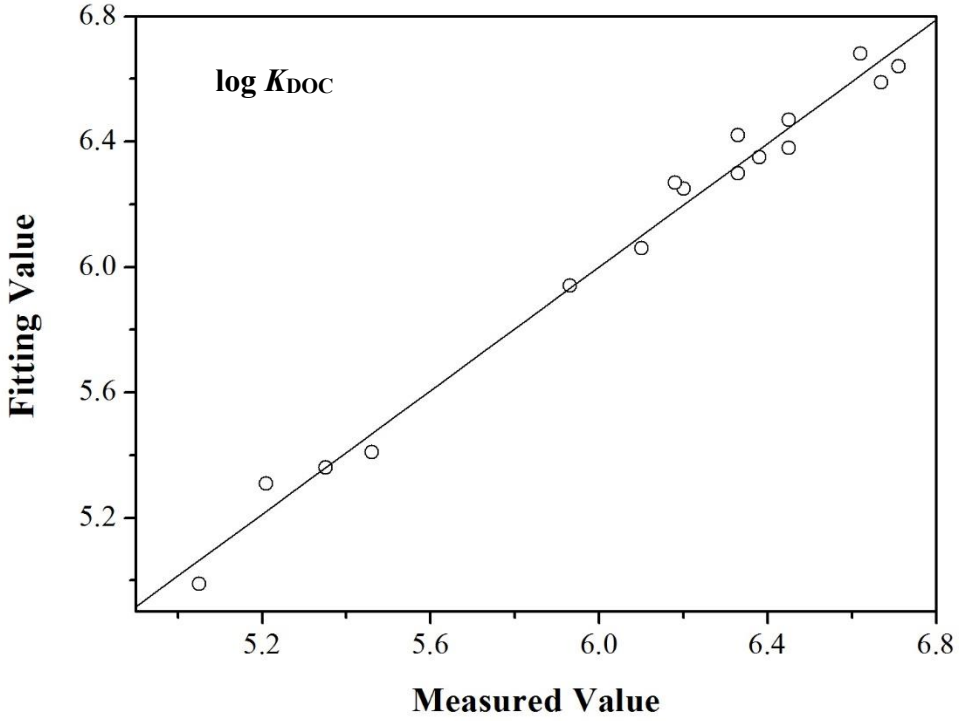

Figure 2-7 Scattergram of log K_{DOC} between measured and fitting value, and the related linear relationship with R^2 of 0.9863 and $p < 0.0001$.

Chapter 3 Anaerobic degradation of poly-brominated diphenyl ether contaminated in products: effect of temperature on degradation characteristics

3.1 Introduction

In a typical practical municipal solid waste anaerobic digestion plant, mechanical sorting is applied to the influent feedstock to separate the biodegradable and non-biodegradable components (Farrell & Jones, 2009; Wei et al., 2017). However, plastics are often mixed into the digester as contaminants, including bags and containers (Suominen et al., 2014). These potentially hazardous materials are thus transferred into the sludge for digestion. Persistent organic pollutants s in the water system, such as polycyclic aromatic hydrocarbons and PCBs can generally be removed under anaerobic conditions (Luo et al., 2016; Siebielska & Sidelko, 2015). Taking advantage of the same methodology, researchers first reported that BDE-209 can be degraded through reductive debromination by microorganisms in anaerobic conditions (Gerecke et al., 2005). Compared with the study of a single substrate, the addition of halogenated electron acceptors, such as trichloroethene (Lee & He, 2010) or PCB (Song et al., 2015), to the reaction system could enhance the PBDE degradation efficiency. To increase PBDE degradation, anaerobic digestion has been combined with the NZVI reduction method, by providing adequate electron donors (Kim et al., 2012; Yang et al., 2017). In addition to the above, biochar has served as an electron shuttle to increase electron transfer efficiency in the reductive debromination of PBDE (Chen et al., 2018a). Using 16S ribosomal RNA (16S rRNA) genes, BDE-99 and BDE-209 were employed as substrates to determine the categories of community during the anaerobic degradation process (Huang et al., 2019; Yan et al., 2017). However, to date, all previous anaerobic digestion research has focused on PBDE degradation under mesophilic conditions, and no research into the temperature effect has been reported thus far. The activity of the reactants can of course be improved by suitably raising the temperature. It is hypothesized that the efficiency of degradation of BDE-209s can be enhanced by thermophilic anaerobic digestion, which has not yet been reported before.

In this study, a 200-day degradation experiment was carried out using a consumer-use curtain containing approximately 10% BDE-209 as the substrate. During the degradation, the volume of methane generated was recorded and the BDE-209 degradation efficiency was

measured. The research results will be useful for developing a better understanding of BDE-209 degradation and methane generation during anaerobic digestion under different temperature and pH conditions.

3.2 Materials and Methods

3.2.1 Materials and study preparation

All the chemical reagents in the experiment, unless otherwise described, were of analytical grade and purchased from Wako Co., Japan.

Both thermophilic and mesophilic anaerobic seed sludge, fed with food waste, were obtained from a previous study. They were cultivated in a SDSAR with a volume of 10 L and a hydraulic retention time of 15 days under thermophilic and mesophilic conditions, respectively (Hu et al., 2018b). The sludges were then cultivated in two sealed 1-L bottles with a 500-mL gas bag connected. Each was placed in a 55 °C or a 35 °C incubator. The organic loading rate was 1 g of glucose every week as the substrate for sludge cultivation. The gas generation volume was recorded every two days. The cultivation process lasted approximately 2 months.

To model actual wastewater conditions, a consumer-use curtain was chosen as the BDE-209 resource to make artificial zymotic fluid. To enhance the distribution and hydrolysis of BDE-209, the curtain was ground in a cryogenic grinder (6870 Freezer/Mill, SPEX™ SamplePrep Inc., USA) (Zhang et al., 2016). First, the curtain was cut into 1 cm × 1 cm square slices. These were then placed in a sealed cryogenic grinding vial with a weight of less than 0.2 g. The vial was then immersed in liquid nitrogen and shaken with 3 cycles, consisting of 5 min pre-cooling, 2 min running and 3 min cooling. The curtain powder was collected and stored at room temperature.

To dilute the sludge to a suitable food-microorganism (F/M) ratio, and to buffer the digestion broth, an artificial inorganic salt solution was prepared before the formal activity assay, which contained (per liter) $MgCl_2 \cdot 6H_2O$, 1000 mg; $CaCl_2 \cdot 2H_2O$, 188 mg; $FeCl_2 \cdot 4H_2O$, 35 mg; NH_4Cl, 1250 mg; K_2HPO_4, 348 mg; KH_2PO_4, 70 mg; $NaHCO_3$, 4000 mg; cysteine·H_2O·HCl, 500 mg; $CoCl_2 \cdot 6H_2O$, 17 mg; $ZnCl_2$, 7 mg; H_3BO_3, 6 mg; $MnCl_2 \cdot 4H_2O$, 61 mg; $NiCl_2 \cdot 6H_2O$, 4 mg; $CuCl_2 \cdot 2H_2O$, 2.7 mg; $NaMoO_4 \cdot 2H_2O$, 2.5 mg; ethylenediaminetetraacetic acid (EDTA), 12.5 mg. After magnetic stirring and ultrasonic dispersion, the prepared solution was stored in a refrigerator at 4 °C.

3.2.2 Activity experiments

After two months of cultivation, the gas production of the seed sludge stabilized. Supplementation with the carbon source was then halted for one week to ensure that as much of the excess substrate as possible was consumed. Fifty-six glass serum bottles with a volume of 120 mL were used for the formal activity assay. The specific experimental conditions for each bottle are listed in Table 1, and the experiments were duplicated twice. After quantifying the weight of the curtain powder, 40 mL of the cultivated seed sludge solution and 40 mL of artificial inorganic salt solution were added to the bottles and mixed together, leaving 40 mL of headspace. After the serum bottle had been capped and sealed, 5 M HCl and NaOH solution were used to carefully adjust the pH of each sample using a syringe (Table 3-1); N_2 was then fed into the headspace of each bottle for 2 min to purge the oxygen. Finally, Na_2S solution (0.2 $mol \cdot L^{-1}$, 1 mL) was injected to remove any residual oxygen. The sealed bottles were then placed in two separate incubators at temperatures of 55 °C and 35 °C, where they were shaken at 120 rpm.

During the degradation process, the volume and composition of the generated gas in the headspace were extracted and analyzed using a gas chromatograph (GC) (GC-8A, Shimadzu Inc., Japan) at the appropriate time, then corrected to standard volume and recorded.

3.2.3 Analysis of PBDEs

After degradation for 200 days, 10 mL of degraded solution containing PBDEs was extracted and lyophilized for 72 hours. The PBDEs in each sample were subjected to the following procedures, modified from previous research (Matsukami et al., 2017).

The first round of extraction (separate soluble organic matter from dried samples): A stainless steel extraction column was packed with 200 mL acetone and hexane mixture solution (1:1 v/v), 0.3 g dried sample and 6 g of Na_2SO_4. The PBDEs were then extracted from the column using a high-speed solvent extractor (SE-100, Mitsubishi Chemical Analytech Co. Ltd., Japan) using toluene as the solvent at 80 °C and under a pressure of 2.0 MPa.

The second round of extraction (rough separation of PBDEs): Using a rotatory evaporator, the 1st extracted PBDEs were concentrated in a 50-mL glass bottle, and then dissolved in 20 mL hexane. The extraction column was filled with the following components from bottom to top: 0.3 g DX gel, 3 g 2% KOH silica, 0.3 g DX gel, 4.5 g 44% H_2SO_4 silica, 6 g 22% H_2SO_4 silica, 0.3 g DX gel, and 1g Na_2SO_4. To extract the PBDEs, 70 mL 5% dichloromethane in hexane (DCM/HEX) was used as the mobile phase.

The third round of extraction (PBDEs solid phase extraction): Utilizing a rotatory evaporator at 36 °C, the 2nd extracted solution was concentrated to a volume of less than 1 mL. An active carbon-dispersed silica gel reversible column (Cat 01894-96, Kanto Chemical Co. Inc., Japan) was used for the solid phase extraction with 80 mL 25% DCM/HEX solution as the mobile phase.

GC-EI-QMS analysis: After evaporation at 36 °C and nitrogen drying, 100 μL hexane was added to the concentrated 3rd extraction solution. The prepared sample was then examined using a GC-EI-QMS system (5975C GC/MSD system, Agilent Technologies Inc., USA) equipped with a 15 m × 0.25 mm × 0.1 μm capillary column (DB-5MS, Agilent Technologies Inc., USA). Twenty-six categories of PBDEs (AccuStandard Inc., USA) were set as the chemical standard reagents during the analysis. The limits of quantification for all samples were in the ranges of 0.02-0.09 $ng \cdot g^{-1}$ for PBDE congeners.

3.2.4 Other analyses

TS and VS were analyzed according to the U.S. EPA Standard Method. The calculated and analyzed TS and VS before and after the activity assay are recorded in Table 3-2.

3.2.5 Statistical analyses

The average increasing rate of high temperature to medium temperature is calculated based on experimental results.

3.3 Results and Discussion

3.3.1 BDE-209 degradation rate

Figures 3-1 and 3-2 show the main composition of PBDEs after 200 days of anaerobic degradation, including BDE-209, nonabromodiphenyl ether (nona-BDE), octabromodiphenyl ether (octa-BDE), and heptabromodiphenyl ether (hepta-BDE). Almost no PBDEs with fewer than 7 bromine atoms were detected. Except for the 7.5-mg mass dosing experiment, all the results showed the decrease in mass of BDE-209 under thermophilic conditions to be greater than under mesophilic conditions: this supports our original hypothesis. Typically, due to the electronegativity of the chloride atoms and overall electron cloud density, the dehalogenation sequence of PCBs is in the order of meta-, para-, and ortho-position (Tiedje et al., 1993).

However, the experimental results showing higher generation of BDE-206, BDE-207 and BDE-208 reveal that the main contribution is from ortho-bromides, which differ from PCBs as to dehalogenation order. The difference between PCBs and BDE-209s is likely attributable to the larger atomic radius of bromine atom than that of chlorine, making the benzene ring overcrowded. The effect of steric hindrance outweighs that of electron density in the molecule. The results of the initial mass dosing and pH effect experiment both illustrate that the mass of generated products among nona-, octa-, hepta-BDE varies in order of magnitude, which illustrates that the debromination reactions are completed one bromine atom at a time, confirming the previously-observed phenomenon (Lee & He, 2010; Robrock et al., 2008). The outcome of the previous stage providing the raw material for the next anaerobic biochemical reaction, which was also affected by reaction temperature, was supported by the observation that trace hepta-BDE directly limited the probability of generation of PBDEs with fewer bromine atoms, which are not detected by GC-EI-QMS.

Even though the overall BDE-209 degradation efficiency is not high, at less than 5% with an average mass reduction rate of 0.8 $\mu g \cdot day^{-1}$, it was a little lower than the results of previous research for five low brominated diphenyl ethers with an initial concentration of 1 $\mu g \cdot mL^{-1}$ (Yen et al., 2009). Furthermore, not only BDE-209 but also highly brominated congeners' degradation pathways were observed to have relatively slow anaerobic degradation rates (Robrock et al., 2008). With the initial high dosing mass of BDE-209, the degradation rate of BDE-209 rocketed, almost fitting the linear relationship between the 2.5 and 10.0 mg dosing mass. Even though BDE-209 has low solubility, the curtain grinding process, combined with the solubilization effect of the dissolved organic carbon in the digestate, appeared to raise the concentration of BDE-209 (Katsoyiannis & Samara, 2006; Kuivikko et al., 2010). This way, the anaerobic digestion system was provided with enough BDE-209 molecules, with the result that the concentration of the substrate increased with dosing mass, which improved the collision probability between the anaerobic microorganisms and BDE-209, enhancing the degradation rate. However, in light of the limited solubility and low hydrolysis of PBDEs (Kuramochi et al., 2007), the trend of increasing BDE-209 degradation rate with increasing mass cannot be maintained: evidence of this is provided by the slowing of growth rate at above 10.0 mg of initial dosing mass, illustrating that there is a distinct load placed on the microorganisms that degrade BDE-209. Nevertheless, if the initial BDE-209 dosing mass is less than 5.0 mg, no hepta-BDEs can be detected in the activity experiment, such as BDE-183, BDE-196 and BDE-197. Assuming sufficient PBDEs, the anaerobic reaction can be accelerated by thermophilic

conditions. On the other hand, high temperatures increase the reaction rate and enrich the products, according with the obvious presence of BDE-202 under thermophilic conditions.

All the pH effect activity experiments were carried out with an initial BDE-209 dosing mass of 10.0 mg. At pH 7, the anaerobic reaction for PBDE removal functions at maximum efficiency, other than the BDE-183 generation rate, owing to measuring variability. Almost all the solutions showed increased pH after 200 days' activity, as illustrated in Table 3-2. Considering the BDE-209 dosing mass in the experiment, the degree of pH variability should contribute to anaerobic digestion: this will be discussed later. Excessive acidity of the solution directly inhibits microbial activity, slowing the degradation rate of PBDE. However, excess alkalinity restricts the amount of hydrogen ions, impeding hydrogenation to some extent during the debromination process. Consequently, irrespective of whether the digestate solution becomes acidic or alkaline, the BDE-209 degradation rate gradually decreases. Even though the acidity of the solution has some influence on the PBDEs degradation rate, the difference in digestion temperature has the greatest effect.

3.3.2 Methane generation

Figures 3-3 and 3-4 exhibit the calculated standard methane volume as a function of the anaerobic digestion process during the 200 days' reaction.Because of the residual substrate, undepleted by the progress of fermentation, the methane generation volumes of the non-curtain sample at pH 7.0 over 200 days under thermophilic and mesophilic conditions are approximately 55 mL and 30 mL, respectively.

Among the thermophilic condition samples, the total volume of generated gas volume steadily increased with curtain dosing masses of 25 mg to 125 mg, providing a close to linear relationship. Considering the debromination of BDE-209 degradation in isolation, the excess gas should contribute to the non-PBDE components of the curtain. Nevertheless, even with the increasing mass of BDE-209, the volume of methane remained stable, resulting in a relatively low total gas volume. In Table 3-2, it can be clearly seen that except for slight fluctuations attributable to analysis error, the average level of both TS and VS for the thermophilic samples are lower than those for the mesophilic samples, which should be contributed to the sludge categories (Hu et al., 2018b). For both the thermophilic and mesophilic samples, after curtain addition, the VS of samples increased with the growth of substrate dosing mass, which is in accordance with the BDE-209 degradation efficiency, even though very little gas was generated under mesophilic conditions.

With the elapse of time, the volume of generated methane increased, and the pH rose. It should be noted that the zeta potentials for all the samples are almost the same, meaning that the surface charges on the samples after degradation are at the same level. For the thermophilic samples at pH values of 6.0-7.5, in the first 30 days, the gas generation rate decreased with increasing alkalinity. The methane volume then stabilized as the pH gradually increased with the continuation of the reaction (Table 3-1). However, there is little gas production for the first 75 days at an initial pH of 5.5 because microbial activity is reduced at lower pH: digestion started after the alkalinity increased, as in the other samples. Nevertheless, the total methane gas volume after the reaction is still very low because of the initial low pH, which is evidenced by the high content of TS and VS after digestion. With the mesophilic samples, because the volume of generated methane is small, there was hardly any significant difference among the samples with different initial pH, which is similar to the results from the no curtain addition samples under thermophilic conditions.

3.3.3 Mechanism of the overall reaction

All the results demonstrated that a faster rate of BDE-209 degradation and better efficiency of methane generation could be achieved via high temperature anaerobic digestion. During the 200 days of anaerobic digestion, part of the non-PBDE component of the curtain serves as a substrate, which is digested into methane and carbon dioxide with the help of active microorganisms. However, the residual part of the non-PBDE component of the curtain, such as organic high molecular polymers left in the solution, cannot be directly decomposed. Meanwhile, BDE-209 molecules in the digestate were adsorbed by the DOC (dissolved organic carbon) substances in the shaking bottles (Wei-Haas et al., 2014). Anaerobic degradation of other organic matter contributed most to the production of electrons, and microorganisms were able to remove only a few bromine atoms from BDE-209. The reactions illustrated above influence each other in various ways as part of the overall mechanism.

3.3.4 Significance of this research

Anaerobic digestion can be used for simultaneous BDE-209 degradation and methane generation. The results of this study demonstrate that high temperatures can enhance the degradation rate of PBDEs, which should contribute to the high reaction activity. The most favorable conditions for the reaction were also determined. Our findings could raise the prospects for the application of anaerobic digestion-based techniques to the degradation of

brominated flame retardants.

3.4 Summary

In this study, the results of the 200-day activity experiment for PBDEs degradation can be summarized as follows: through both mesophilic and thermophilic anaerobic digestion, BDE-209s were successfully degraded into PBDEs with less bromine atoms. And non-BDE parts of the curtain were decomposed into methane and carbon dioxide. The BDE-209 degradation rate of the thermophilic reactor is significantly higher than that of the mesophilic rate. Furthermore, even at the same cultivation temperature, the degradation rate is higher with the initial BDE-209 dosing mass, and the optimal pH for anaerobic degradation is 7.0

Table 3-1 The temperature, pH, initial curtain dosing mass for each experiment.

No	Group	Temperature (°C)	pH		Curtain powder mass (mg）	
			Predicted	Actual	Predicted	Actual
1	Objective	55 ± 0.5	7.00	7.05 ± 0.05	100.00	100.30 ± 0.30
2	Concentration effect	55 ± 0.5	7.00	7.15 ± 0.05	125.00	124.25 ± 0.25
3	Concentration effect	55 ± 0.5	7.00	7.10 ± 0.10	75.00	74.70 ± 0.50
4	Concentration effect	55 ± 0.5	7.00	7.10 ± 0.00	50.00	50.10 ± 0.40
5	Concentration effect	55 ± 0.5	7.00	7.10 ± 0.00	25.00	25.30 ± 0.30
6	pH effect	55 ± 0.5	5.50	5.50 ± 0.10	100.00	99.35 ± 0.25
7	pH effect	55 ± 0.5	6.00	6.20 ± 0.00	100.00	99.50 ± 0.40
8	pH effect	55 ± 0.5	6.50	6.45 ± 0.05	100.00	100.50 ± 0.60
9	pH effect	55 ± 0.5	7.50	7.45 ± 0.05	100.00	99.80 ± 0.30
10	No substrate effect	55 ± 0.5	7.00	7.15 ± 0.05	-	-
11	No substrate effect	55 ± 0.5	5.50	5.40 ± 0.10	-	-
12	No substrate effect	55 ± 0.5	6.00	6.10 ± 0.10	-	-
13	No substrate effect	55 ± 0.5	6.50	6.45 ± 0.05	-	-
14	No substrate effect	55 ± 0.5	7.50	7.45 ± 0.05	-	-
15	Temperature effect	35 ± 0.5	7.00	7.00 ± 0.00	100.00	99.45 ± 0.05
16	Temperature effect	35 ± 0.5	7.00	6.95 ± 0.05	125.00	124.90 ± 0.20
17	Temperature effect	35 ± 0.5	7.00	6.90 ± 0.05	75.00	74.35 ± 0.30
18	Temperature effect	35 ± 0.5	7.00	7.00 ± 0.00	50.00	49.85 ± 0.55
19	Temperature effect	35 ± 0.5	7.00	7.10 ± 0.10	25.00	24.65 ± 0.35
20	Temperature effect	35 ± 0.5	5.50	5.30 ± 0.00	100.00	100.05 ± 0.05
21	Temperature effect	35 ± 0.5	6.00	6.05 ± 0.05	100.00	99.90 ± 0.60
22	Temperature effect	35 ± 0.5	6.50	6.40 ± 0.00	100.00	99.80 ± 0.80
23	Temperature effect	35 ± 0.5	7.50	7.50 ± 0.10	100.00	100.40 ± 0.00
24	Temperature effect	35 ± 0.5	7.00	7.05 ± 0.05	-	-
25	Temperature effect	35 ± 0.5	5.50	5.45 ± 0.05	-	-
26	Temperature effect	35 ± 0.5	6.00	5.95 ± 0.05	-	-
27	Temperature effect	35 ± 0.5	6.50	6.40 ± 0.00	-	-
28	Temperature effect	35 ± 0.5	7.50	7.40 ± 0.00	-	-

Table 3-2 The pH, zeta potential, TS, and VS after 200 days of anaerobic digestion.

No	pH	zeta potential (mV)	TS ($mg \cdot L^{-1}$)	VS ($mg \cdot L^{-1}$)
1	7.54 ± 0.07	-15.15 ± 0.05	6000.0 ± 52.5	4337.5 ± 52.5
2	7.47 ± 0.01	-16.80 ± 0.00	6718.7 ± 2.5	5006.3 ± 81.3
3	7.48 ± 0.01	-19.20 ± 0.00	5800.0 ± 37.5	4306.3 ± 37.5
4	7.51 ± 0.02	-16.15 ± 0.05	5562.5 ± 2.5	4112.5 ± 87.5
5	7.49 ± 0.01	-16.20 ± 0.00	5425.0 ± 2.5	3787.5 ± 6.2
6	6.55 ± 0.07	-14.20 ± 0.00	8793.7 ± 16.2	5181.2 ± 93.7
7	7.12 ± 0.02	-15.40 ± 0.00	5575.0 ± 70.0	3843.7 ± 75.0
8	7.25 ± 0.02	-17.10 ± 0.10	5350.0 ± 55.0	3425.0 ± 81.3
9	7.58 ± 0.00	-16.65 ± 0.05	5850.0 ± 75.0	3331.2 ± 62.5
10	7.55 ± 0.05	-13.90 ± 0.00	5497.5 ± 87.5	3406.2 ± 2.5
11	6.66 ± 0.05	-13.20 ± 0.00	5750.0 ± 62.0	3537.5 ± 18.8
12	7.06 ± 0.00	-14.85 ± 0.05	5491.3 ± 81.3	3681.2 ± 43.8
13	7.20 ± 0.03	-12.20 ± 0.00	5531.2 ± 18.7	3637.5 ± 37.5
14	7.60 ± 0.01	-14.80 ± 0.00	5031.3 ± 58.8	3458.5 ± 18.8
15	7.21 ± 0.10	-13.15 ± 0.05	8112.5 ± 68.7	6325.0 ± 25.0
16	7.15 ± 0.10	-10.25 ± 0.05	8881.2 ± 50.0	7118.7 ± 68.8
17	7.20 ± 0.01	-10.15 ± 0.05	8125.0 ± 6.3	6681.3 ± 6.2
18	7.22 ± 0.02	-10.20 ± 0.00	8181.2 ± 0.0	6656.2 ± 10.0
19	7.25 ± 0.05	-10.35 ± 0.05	7250.0 ± 37.5	6437.5 ± 30.0
20	6.32 ± 0.01	-12.70 ± 0.00	8262.5 ± 75.0	6012.5 ± 62.5
21	6.75 ± 0.02	-10.55 ± 0.05	7950.0 ± 57.5	6600.0 ± 68.7
22	6.89 ± 0.00	-13.95 ± 0.05	8025.0 ± 6.2	6668.7 ± 18.8
23	7.31 ± 0.03	-15.10 ± 0.00	8981.3 ± 6.3	6768.8 ± 25.0
24	7.15 ± 0.05	-14.20 ± 0.00	7475.0 ± 56.3	6037.5 ± 43.8
25	6.42 ± 0.01	-13.90 ± 0.00	7706.2 ± 31.2	5843.8 ± 81.2
26	6.73 ± 0.02	-14.75 ± 0.05	7318.8 ± 18.8	5912.5 ± 12.5
27	6.91 ± 0.02	-14.30 ± 0.00	7368.8 ± 31.3	5831.3 ± 43.7
28	7.16 ± 0.01	-13.50 ± 0.00	8225.0 ± 37.5	5437.5 ± 50.0

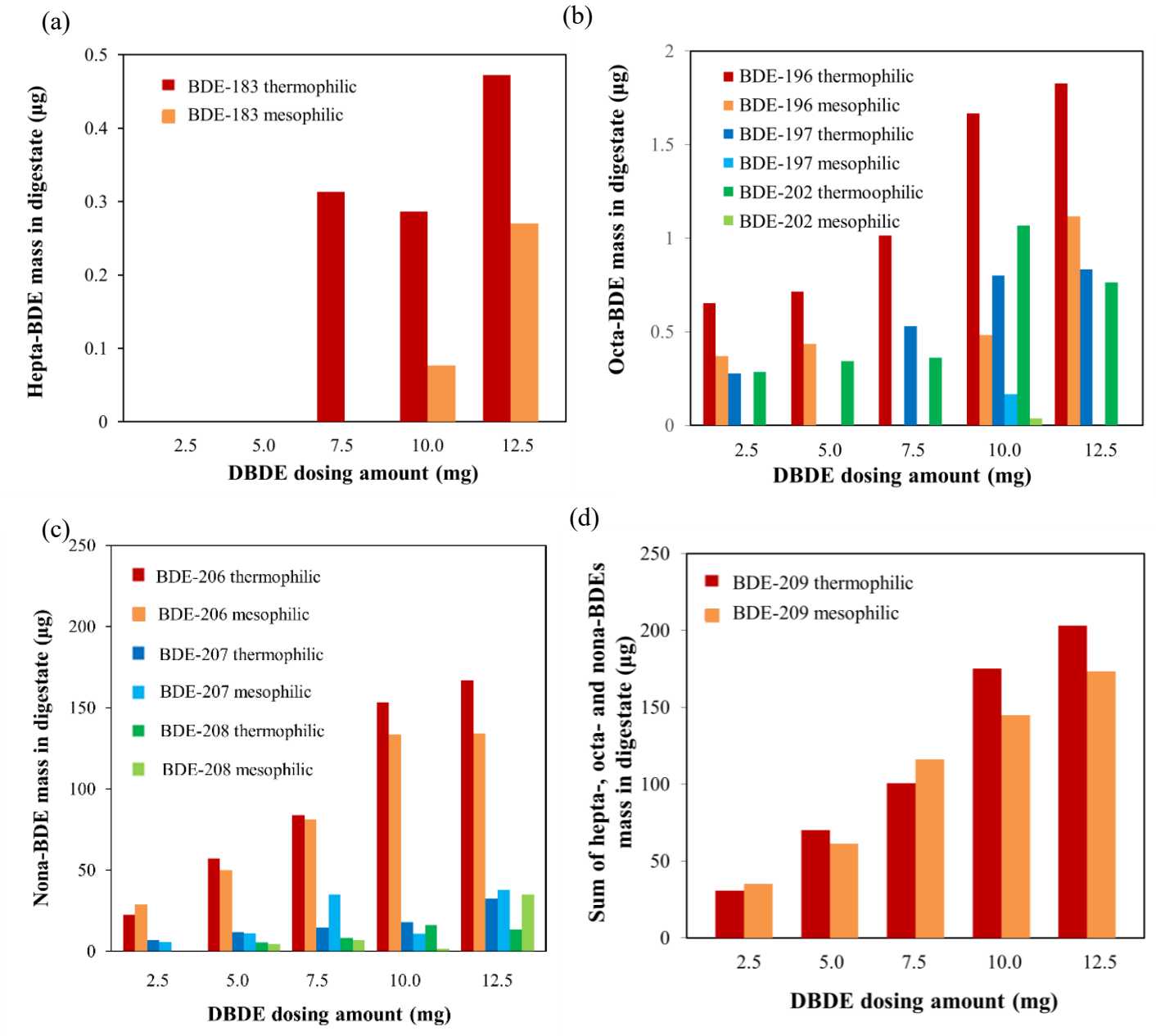

Figure 3-1 The average mass of hepta-BDE (a), octa-BDE (b), nona-BDE (c) and total mass of hepta-BDE, octa-BDE and nona-BDE (d) in digestate after 200 days of anaerobic digestion with different initial BDE-209 dosing mass, under thermophilic and mesophilic conditions.

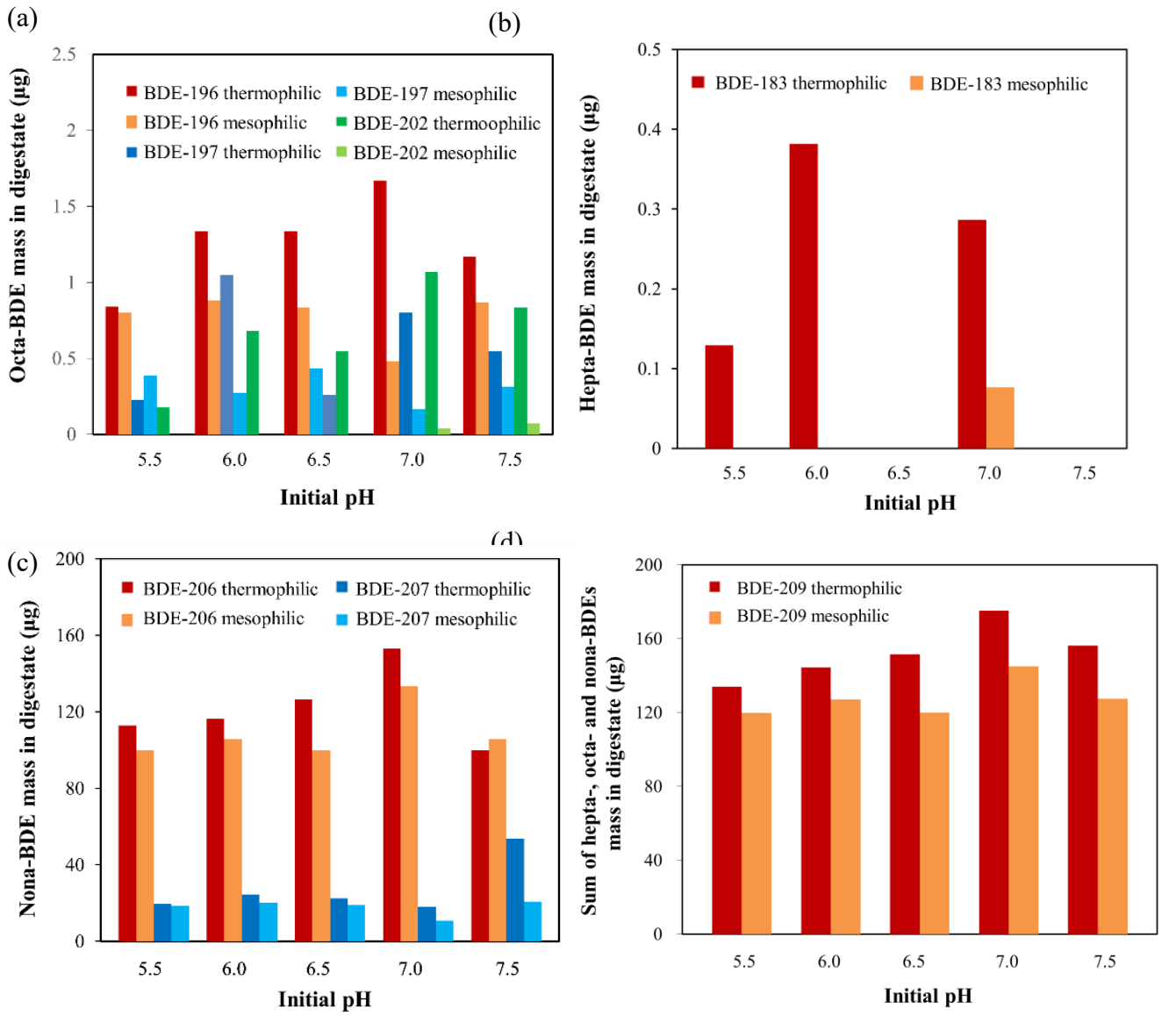

Figure 3-2 The average mass of hepta-BDE (a), octa-BDE (b), nona-BDE (c) and total mass of hepta-BDE, octa-BDE and nona-BDE (d) in digestate after 200 days anaerobic digestion with different initial pH, under thermophilic and mesophilic condition.

(a)

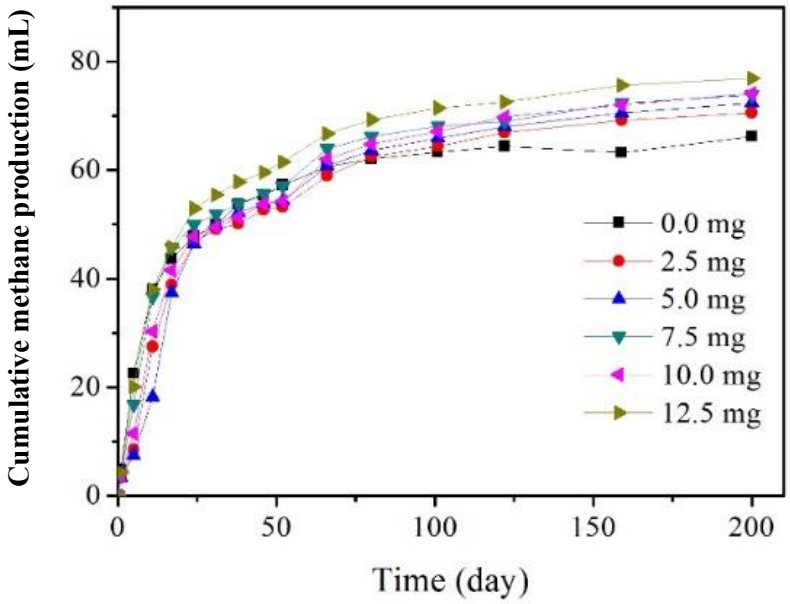

(b)

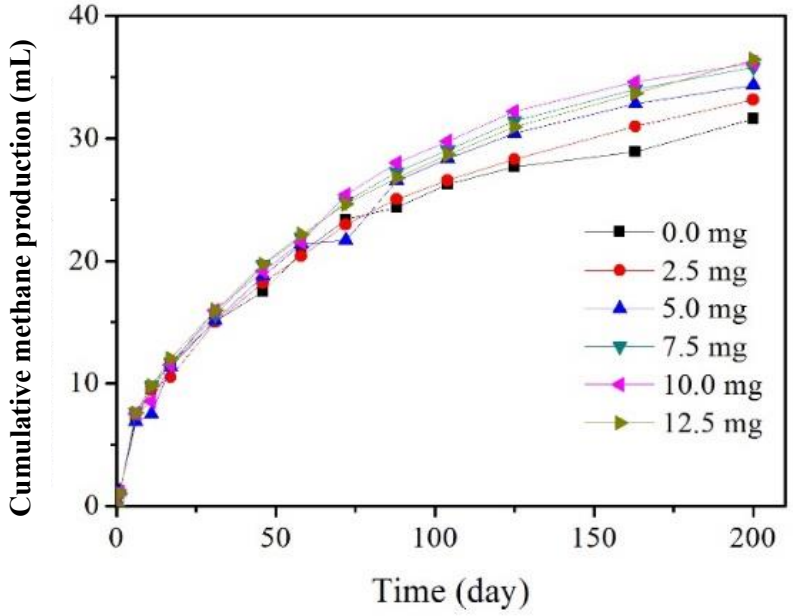

Figure 3-3 The record of total volume for cumulative methane production (calculated to standard) with different initial BDE-209 dosing mass during 200 days anaerobic digestion, under thermophilic (a) and mesophilic (b) condition, respectively.

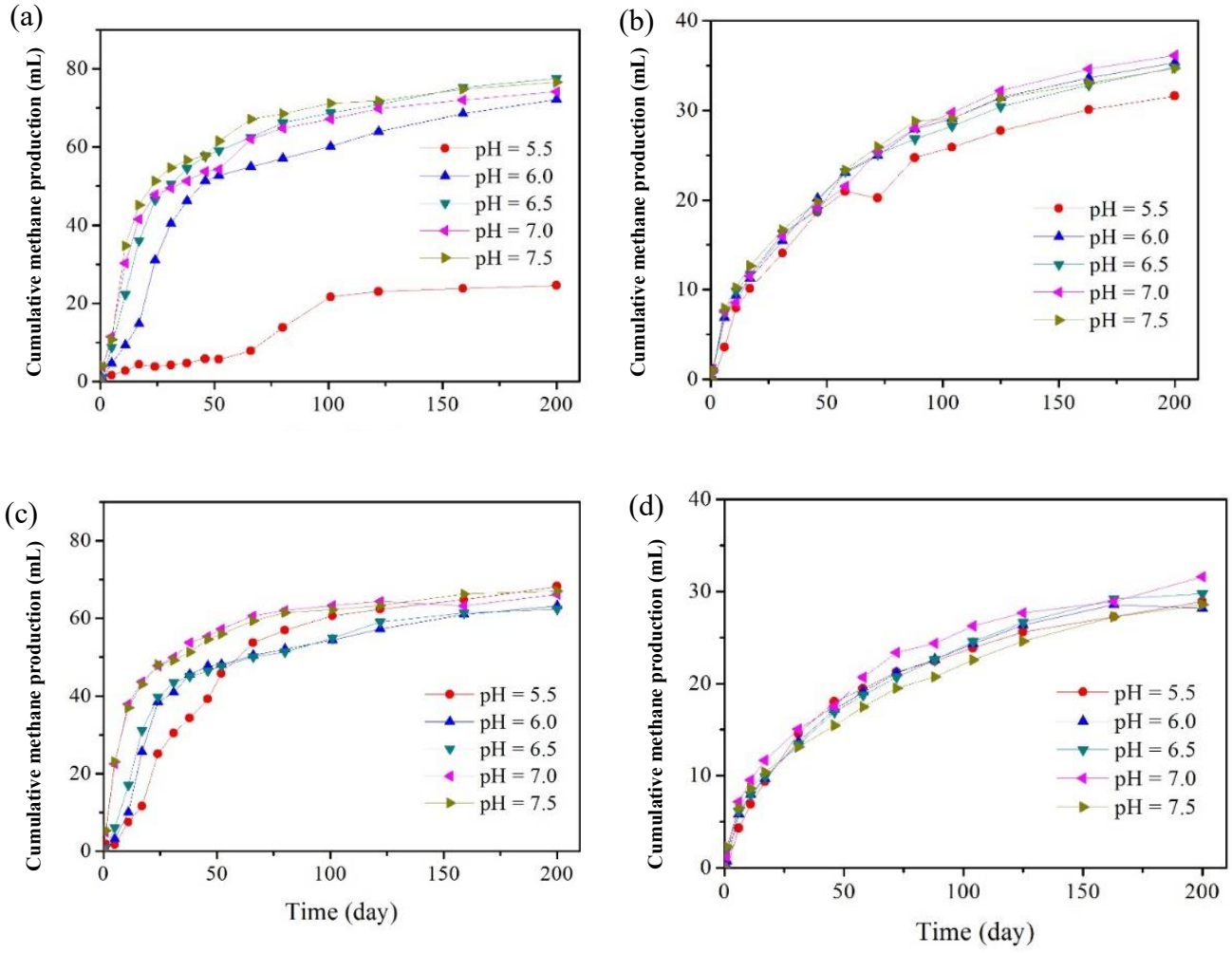

Figure 3-4 The record of total volume for cumulative methane production (calculated to standard) with different pH during 200 days anaerobic digestion, under thermophilic with BDE-209 (a), mesophilic with BDE-209 (b), thermophilic without BDE-209 (c) and mesophilic without BDE-209 (d) respectively.

Chapter 4 Anaerobic degradation pathway of BDE-209 contaminated in products: effect of temperature on degradation characteristics

4.1 Introduction

Typically, the anaerobic degradation of PBDE should be classified as debromination. During the procedure, PBDE accept electrons and protons together, then form PBDEs with less bromine atoms and release free bromide ions into system. Benzene ring from the PBDE frame in this process does not break, which is similar with the nano zero valent iron reduction reaction. Consider the high reaction activity, thermophilic conditions were introduced into the anaerobic digestion. The BDE-209 in sewage sludge should be the most composition of all PBDEs (Knoth et al., 2007). As has strong degradation ability for complex organic compounds, researchers reported that BDE-209 could be degraded through reductive debromination by anaerobic microorganisms under. However, the difference in specific degradation characteristics between these two temperature conditions remains unclear. In this research, we investigated the effects of temperature on BDE-209 anaerobic degradation pathway of PBDEs under anaerobic condition.

In this study, two continuously-stirred anaerobic digesters were applied to carry out the 150 days' anaerobic digestion experiments under thermophilic (55°C) and mesophilic (35°C) conditions, respectively. The experimental results showed that the debromination rate at thermophilic condition was higher than that at mesophilic condition, reaching 0.4 $\mu g \cdot d^{-1}$. In addition, it was found that the thermophilic condition could improve the removal of para- and meta- bromines, although the data have not been normalized. It suggests that thermophilic BDE-209 degradation is more effective than of the mesophilic one. The findings from this work suggest the prospects of applying anaerobic digestion-based techniques for bromide retardant degradation.

4.2 Materials and Methods

4.2.1 CSTR system

A schematic diagram and photographs of the CSTR system applied in this research is shown in Figure 4-1. The whole reactor is mainly composed of three components, body, cover, and stirring device. The material of the reactor for mesophilic (35°C) and thermophilic (55°C)

condition is general and heat tolerant polyvinyl chloride, respectively. And the insulating layer of the reactor is supplied by circulation constant temperature water bath (NTT-20S, Tokyo Rikakikai Co., Ltd., Japan). The inner barrel of the reactor is a cylinder with a diameter of 100 mm and a height of 210 mm, and the volume of it is 1.6 L. There are four sampling port distributed the sidewall of the body. In order to ensure the airtightness of the system, body and upper cover are locked through a rubber ring and eight bolts. On the cover, there is a 500-mL gas bag for collecting methane gas and a filling port for adding substrate, sealed with rubber stopper. There is an agitation system on the top of the reactor, directly driven by a 100 V AC motor (PSH425-401P, Oriental Motor Co., Ltd., Japan), and a 190 mm-length stainless steel stirring bar pass into the reactor body through the top cover. Through the liquid seal from the built-in spout, the intimate atmosphere is isolated from the outside.

4.2.2 Bioreactor experiment

Except special description, all the chemical reactants in this research were of analytical grade, purchased from the Wako co., Japan. Before sludge cultivation and experiment carrying out, liquid leak detection and airtightness were checked.

Artificial inorganic nutrient salt solution was prepared using the formula from previous method. In brief, 1 L solution contained: $NaHCO_3$, 4000 mg; NH_4Cl, 1250 mg; $MgCl_2 \cdot 6H_2O$, 1000 mg; cysteine$\cdot H_2O \cdot HCl$, 500 mg; K_2HPO_4, 348 mg; $CaCl_2 \cdot 2H_2O$, 188 mg; KH_2PO_4, 70 mg; $MnCl_2 \cdot 4H_2O$, 61 mg; $FeCl_2 \cdot 4H_2O$, 35 mg;; $CoCl_2 \cdot 6H_2O$, 17 mg; ethylenediaminetetraacetic acid (EDTA), 12.5 mg; $ZnCl_2$, 7 mg; H_3BO_3, 6 mg; $NiCl_2 \cdot 6H_2O$, 4 mg; $CuCl_2 \cdot 2H_2O$, 2.7 mg; $NaMoO_4 \cdot 2H_2O$, 2.5 mg; $ZnCl_2$, 1 mg. Seed sludge, fed with food-waste, were obtained from a SDSAR under thermophilic and mesophilic situation respectively, which has a volume of 10 L and a hydraulic retention time of 15 days. For sludge cultivation in the CSTR, 700 mL seed sludge and 700 mL artificial water were mixed together with a rotating speed of 10 rpm. Considering the organic loading rate, 0.5 g glucose every 5 days was selected as substrate for the sludge cultivation, and the gas generation volume was recorded every day.

For both thermophilic and mesophilic condition, after approximate 2 month cultivation, the gas production of the sludge became stable, then cut off the carbon source supplement for one week to consume the excess substrate as much as possible. 1 mg BDE-209 (Lot.2VXXI-OK, 95.0% purity, Tokyo Chemical Industry Co. Ltd., Japan) was added into the reactor to carry out the formal experiment, referred from a previous work with a concentration of 0.9 $mg \cdot kg^{-1}$ sludge in the San Francisco Bay. During the degradation process, the volume and composition

of generated gas in the headspace were recorded and analyzed by Gas Chromatography (GC) equipment (GC-8A, Shimadzu Inc., Japan), then calculated to standard volume. Each time, 10 mL BDE-209 degradation solution samples were collected through sidewall port, saved in a 4°C refrigerator.

4.2.3 PBDE measurements

Through multiple extraction processes, the purification of all the samples was followed using the modified method (Guerra et al., 2015). In brief, all the solution samples were compressed into floc status by using freeze-drying (Eyela FDU-1110, Tokyo Rikakikai Co., Ltd., Japan). Secondly, the dried samples were extracted using toluene as solvent and Na_2SO_4 as extraction column in a high-speed solvent extractor (SE-100, Mitsubishi Chemical Analytech Co. Ltd., Japan). Thirdly, the extracted solution was deeply extracted using 5% dichloromethane in hexane as the solvent, DX gel, and silica as the primary extraction column. Then, during the solid-phase extraction process, activated carbon-dispersed silica gel reversible column (Cat 01894-96, Kanto Chemical Co. Inc., Japan) and 25% dichloromethane in hexane were taken advantage to separate the residual impurities. Finally, the extracted PBDE solutions were analyzed using a GC-EI-QMS system (5975C GC/MSD system, Agilent Technologies Inc., USA) equipped with a 15 m × 0.25 mm × 0.1 mm capillary column (DB-5MS, Agilent Technologies Inc., USA)..

4.2.4 Dynamic fitting

A first-order kinetic (Equation 4-1) and second-order kinetic model (Equation 4-2) were used to examine the degradation kinetics (Liu, 2008), which could be described by the following equations:

$$c_t = c_0 \times e^{-k_1 t} \quad (4\text{-}1)$$

$$\frac{1}{C_t} = k_2 t + b \quad (4\text{-}2)$$

where c_t and c_0 ($\mu g \cdot L^{-1}$) are the concentration of PBDEs during the degradation process at reaction time t, respectively, and k_1, k_2 and b are constants.

4.3 Results and Discussion

4.3.1 BDE-209 degradation and other PBDEs generation

The aim of this research is to investigate the temperature effect on BDE-209 anaerobic digestion and try to explain the pathway during the degradation process in an ideal CSTR. It should be admitted that there is a little photolysis and pyrolysis of PBDEs themselves, proved by lots of previous work. However, these effects only take a very small percentage during the whole degradation, which would not influence the subsequent deduction process. All the calculation of increasing or decreasing for the PBDE contain these small parts. Figure 4-2 showed the composition of PBDEs' mass after 200 days' anaerobic degradation, including the nona-, octa-, and hepta-BDE. Similar with previous results that BDE-209 debrominated with a corresponding increase in nona-, octa-, hepta-BDEs (Tokarz et al., 2008). Because the purity of the original BDE-209 reactant is not as high as 100%, there should be some PBDEs with bromide number less than ten. For instance, it is obviously that the average mass of initial BDE-206 and BDE-207 is 125 μg and 40 μg, respectively. With the increase of reaction time, the concentration of nona-BDE in both thermophilic and mesophilic condition enhanced step by step, except the BDE-207 from thermophilic one by the 50 days, which should be contributed to the measurement error. Because of the relative high measurement error form, the low concentration of octa- and hepta-BDE, lower than that of nona-BDE at the magnitude, there is a range of PBDE concentration fluctuation during the degradation process, but the overall trend of concentration change is still increasing. In sum, PBDEs with bromide number less than ten is generated during the anaerobic digestion in the CSTR.

For BDE-206, approximate 200 μg increasing mass from thermophilic condition was presented, higher than that with a 120 μg increasement from mesophilic one. For BDE-207, there is a 30 μg increasement change between initial and final experimental in thermophilic condition, which is 1.5 times higher than that of the mesophilic one. Both phenomena illustrate that the debromination order of BDE-209 is ortho-, meta- position because of the strong steric hindrance effect in the molecular, which fits the previous research. BDE-196 can be generated from both BDE-206 and BDE-207 through meta- and ortho- debromination, respectively. However, BDE-197 can only be obtained through the meta- debormination process from BDE-207. Thus, limited reactant BDE-207, single reaction process, and low speed from meta-position reaction directly restricted the BDE-197 generation, which could be illustrated from the result of the low increasing of BDE-197, compared with that of BDE-196. For the

temperature effects on octa-BDE, the results proved that 7 times concentration of initial BDE-196 is obtained after long-time degradation in thermophilic condition, a little higher than the 6 times in the mesophilic one. And there is almost no big difference of BDE-197 mass enhancement between both thermophilic and mesophilic condition, approximate 5 times enhanced after degradation. For the hepta-BDE, considering its extra low content, the fluctuation of its mass change during the degradation is much more obvious than the nona-BDE and octra-BDE. Even the BDE-183 mass in thermophilic condition by the 45th day is negative. And previous work showed that in sewage from both WWTPs, PBDEs with higher bromide atoms were removed faster than the lower brominated congeners. One exception was tri-BDE, which was degraded completely within 15 months of cultivation, which fits our research results (Stiborova et al., 2015b)

In sum, nona-BDE, octa-BDE and nona-BDE generating rate in the thermophilic condition is higher than that in the mesophilic one. And the average degradation rate for BDE-209 under thermophilic condition is approximate 1.5 $g \cdot day^{-1}$, higher than that with a rate of 0.9 $\mu g \cdot day^{-1}$ under mesophilic one. This phenomenon illustrates that high temperature accelerates the activity of microorganism, then the catalytic activity for BDE-209 degradation increased, which is in accordance with our previous research. Furthermore, compared with typical shaking in previous batch experiment with a maximum degradation rate of 0.8 $\mu g \cdot day^{-1}$, the degradation rate in CSTR is much higher. We speculate that continuous stirring in CSTR enhance the collision ability between microorganism and PBDE molecular, then the number of active sites increased, which improve the catalytic activity for degradation.

During the total degradation process, PBDEs are first dissolved and hydrolyzed in the digestate solution through the dissolved organic carbon, including carbohydrate, protein, lipid end etc. Same as the general adsorption process (Deng & Tam, 2016), dominant dissolved PBDEs would be adsorbed on the cell surface of microorganism. And by hydrogenation and debromination process, BDE-209 could be changed into PBDEs with lower bromide atoms during the long-term degradation time. However, the potential toxicity of PBDEs increased after metabolized to lower brominated forms (Benedict et al., 2007). In this way, with the gradual degradation, the restriction of catalysts activity enhanced, reducing the degradation rate, which could be illustrated from the BDE-209 decreasing mass under mesophilic condition in Figure 4-3.

4.3.2 Methane generation and Kinetic dynamic

Figures 4-3 exhibit the calculated standard methane volume as a function of the anaerobic digestion process during the 210 days' reaction in both CSTR and activity experiment under thermophilic and mesophilic condition. At every temperature, the methane volume continued to increase with the elapse of time, except for some fluctuations of the total methane volume under thermophilic conditions owing to errors caused by frequent measurements of the generated gas. No matter in CSTR or in serum bottles, the rates of gas generation for the thermophilic samples rocketed in the first 30 days, then got slower for 50 days and became stable in the next 130 days, reaching approximate 85 mL per 100 mL sludge. However, for the mesophilic condition, total volume seemed stable after 80 days' slowing increasing, reaching approximate 25 mL per 100 mL sludge. The differences from microorganism activity under two temperature directly contributed to the different gas generating rate. And all the generated methane gas came from the residual substrate, undepleted from the cultivation proceed. There is no methane generated from BDE-209 degradation. From the side, the results revealed that BDE-209 was degraded process into nona-, octa- and hepta-BDE by debromination without aromatic ring structure destruction.

The pseudo-first-order kinetic simulation for the BDE-209 degradation have been given in Figure 4-5. The degradation processes under both thermophilic and mesophilic conditions suited the pseudo-first-order models very well. Especially, the mesophilic one showed a high R^2, higher than 0.95. This result is in accordance with previous research that BDE-209 exhibited a pseudo-first-order degradation with a long half-life of 700 d (Gerecke et al., 2006)

4.4 Summary

In this study, new information was obtained after a 210-day BDE-209 anaerobic digestion experiment in CSTR. High temperature accelerates the activity of microorganism, then the catalytic activity for BDE-209 degradation increased, which is in accordance with results in chapter 3. And through multiple-step reaction, BDE-209 is degraded into, nona-, octa- and hepta-BDEs by debromination process. The anaerobic digestion of BDE-209 between both thermophilic and mesophilic condition fits a first-order reaction kinetics. All these findings suggest the potential of using anaerobic digestion-based techniques for degrading bromide retardant in wastewater treatment.

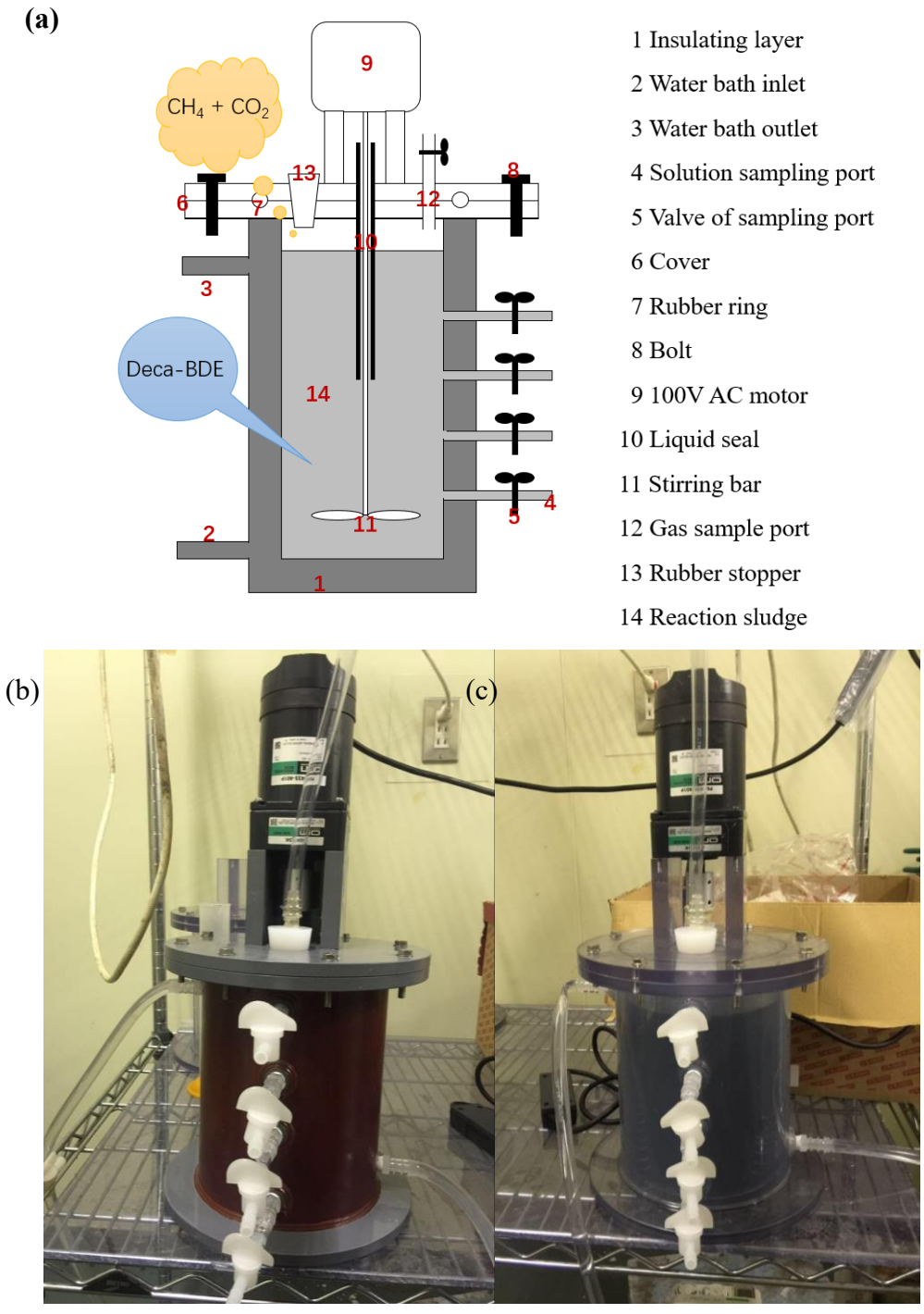

Figure 4-1 The structure figures of CSTR: (a) schematic figure; (b) actual thermophilic reactor; (c) actual mesophilic reactor..

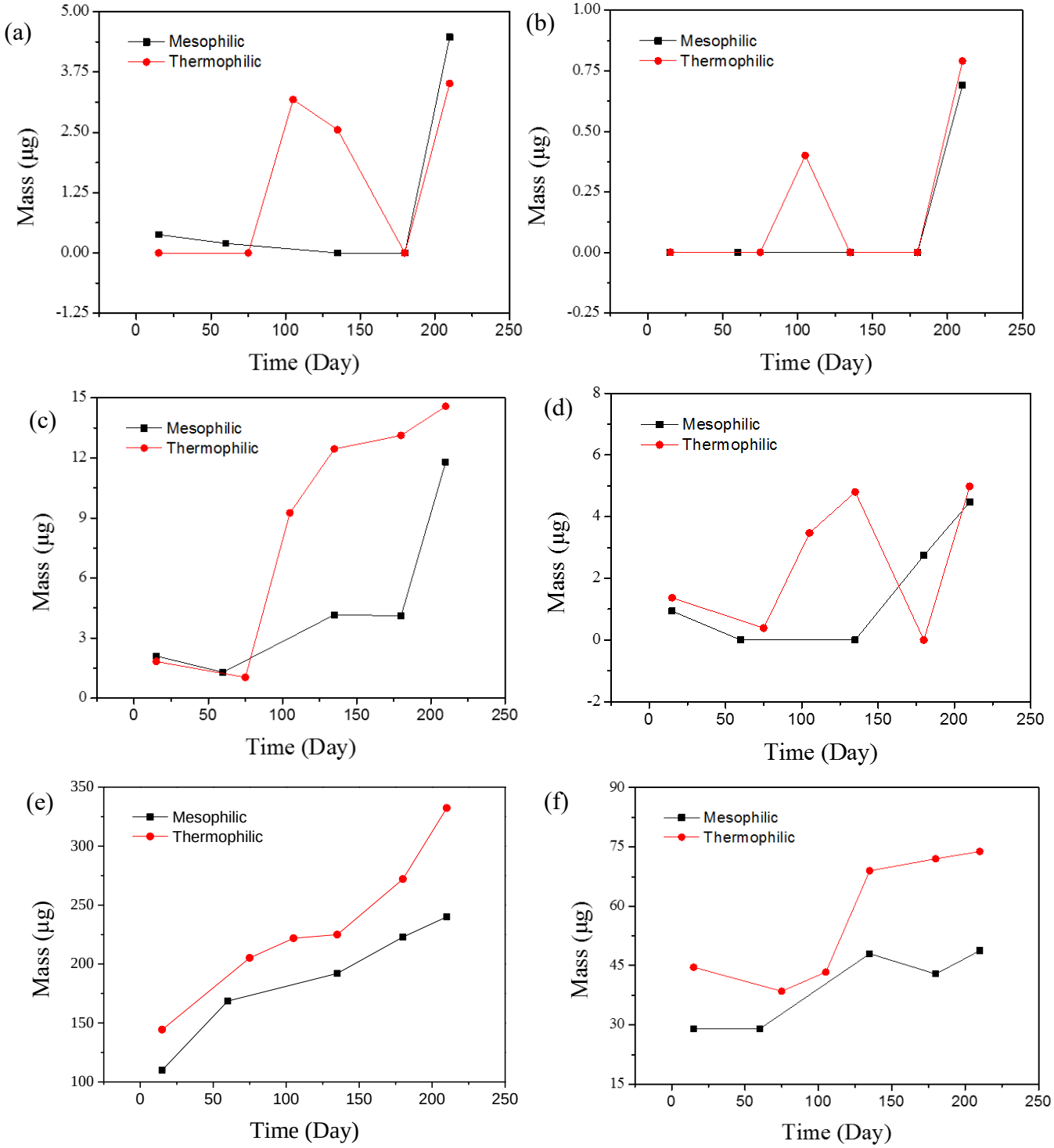

Figure 4-2 The increasing mass of (a) BDE-183; (b) BDE-191; (c) BDE-196; (d) BDE-197; (e) BDE-206; (f) BDE-207 in CSTR by time under thermophilic and mesophilic conditions, respectively.

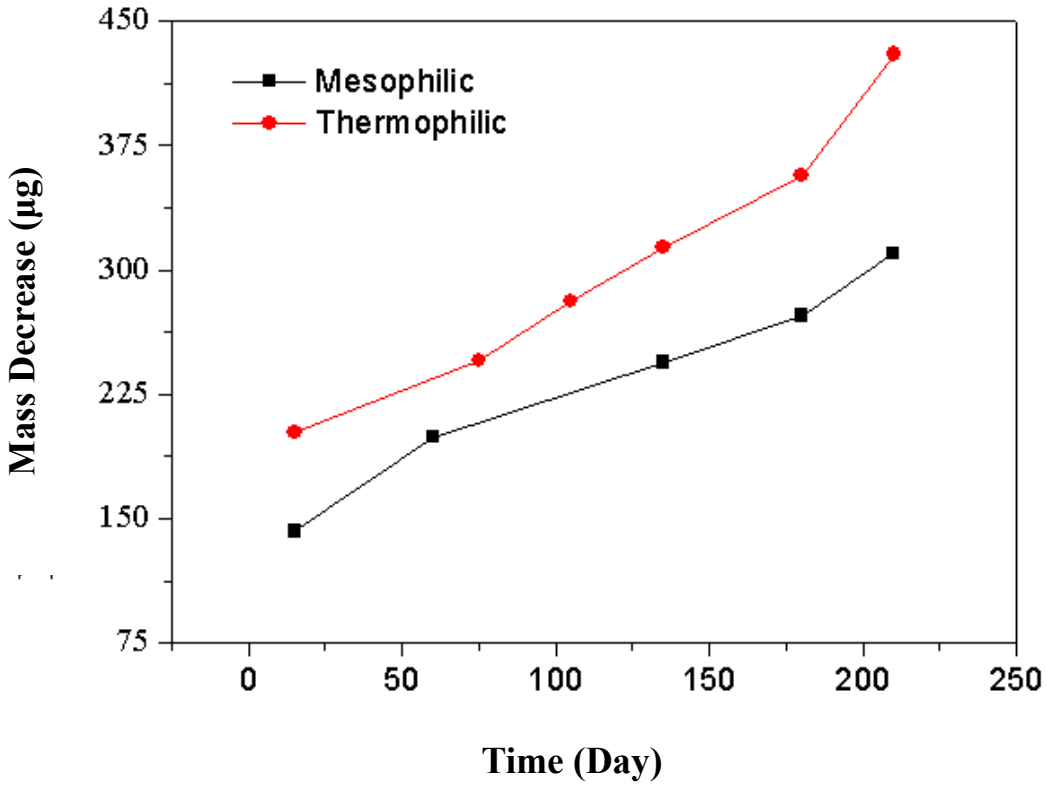

Figure 4-3 The decreasing mass of BDE-209 in CSTR by time under thermophilic and mesophilic conditions, respectively.

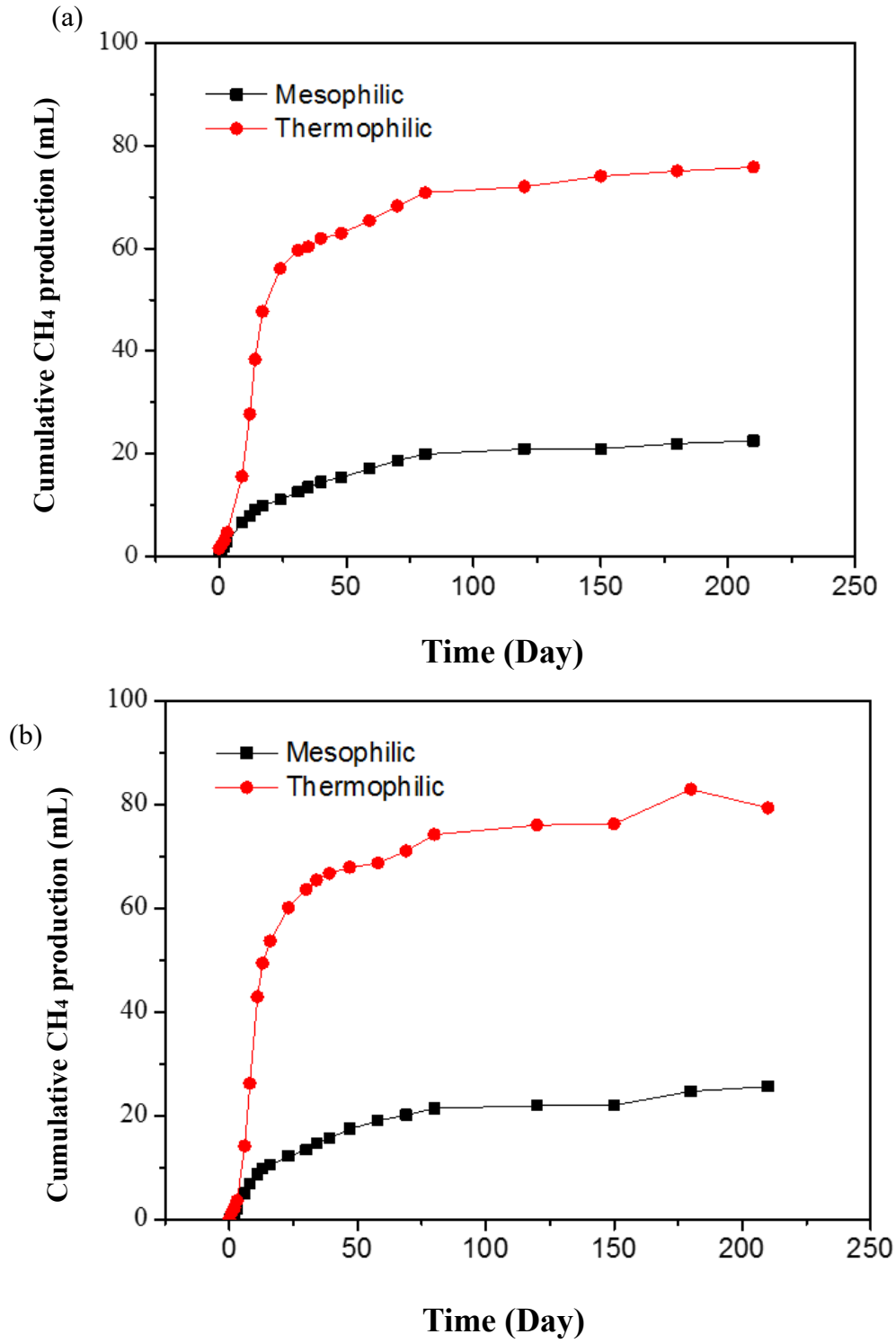

Figure 4-4 The record of total volume for the generated methane (calculated to standard) under thermophilic and mesophilic condition in different reactors: CSTR with volume of 1.6 L (a) and serum bottle with volume of 80 mL (b).

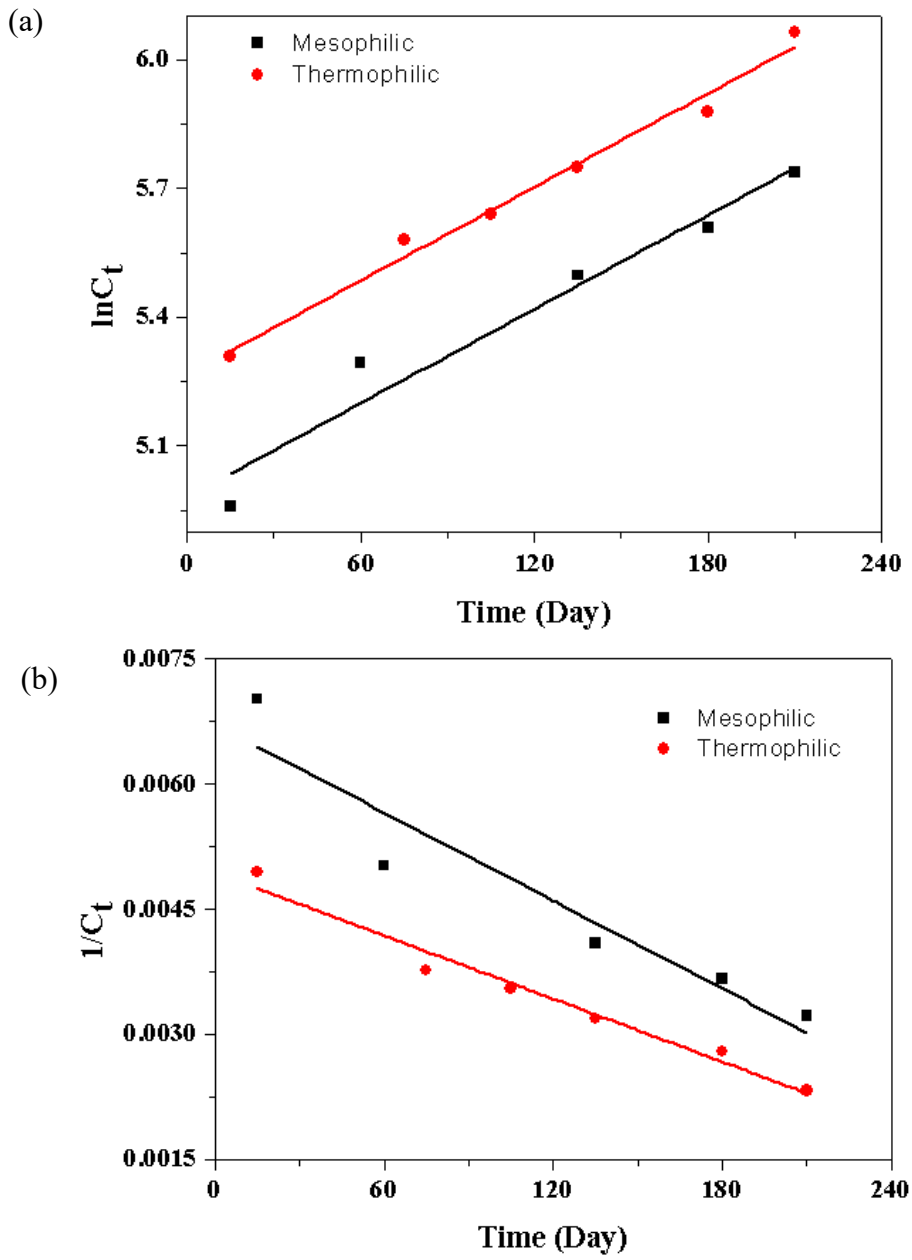

Figure 4-5 Scattergram of kinetics fitting line: pseudo-first-order (a) and pseudo-second-order (b).

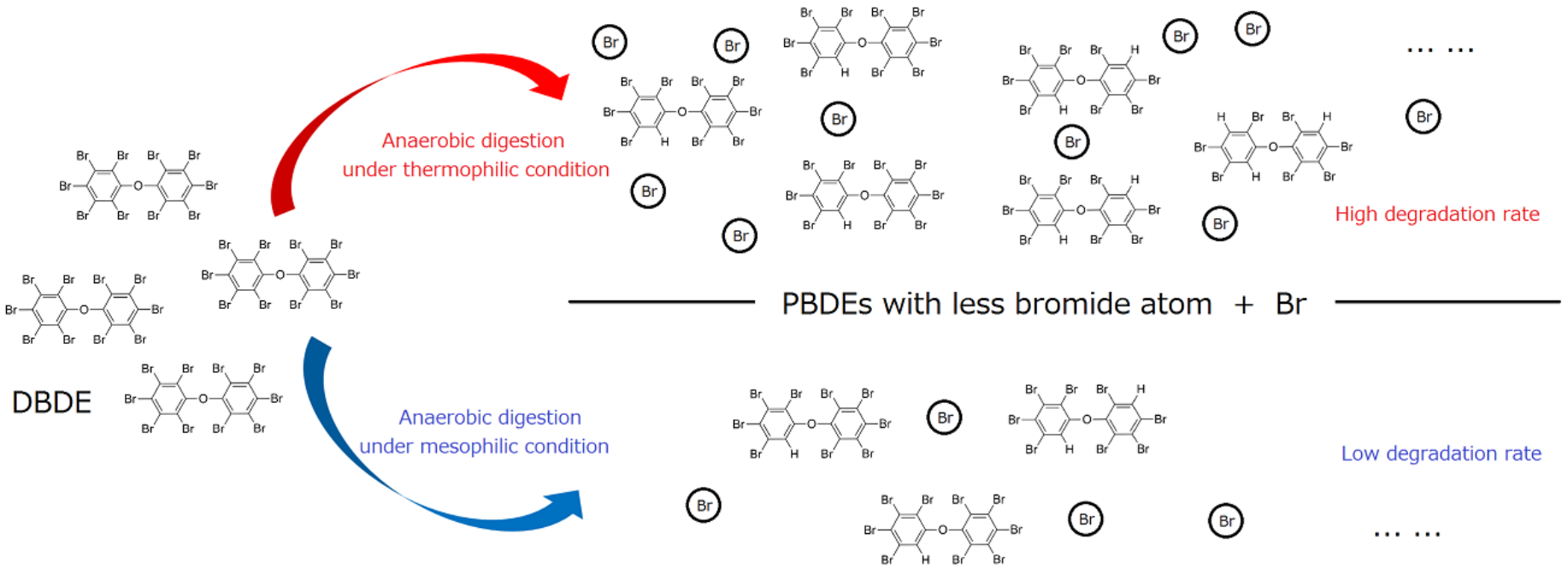

Figure 4-6 The BDE-209 anaerobic degradation pathway in CSTR.

Chapter 5 Conclusions

In this thesis, efforts were made to research the distribution, degradation rate and pathway of PBDEs in anaerobic condition. In the whole anaerobic digestion process, BDE-209 degradation was firstly dissolved in the DOC solution by solubilization effect, then the degradation rate increased with temperature, fitting a first-order reaction kinetics during the multiple-step reactions, which could be illustrated by the followings:

(1) Understand the pollutant's environmental behavior in a similar water system. With the help of FTIR, TG, XRD, zeta potential measuring and a liner regression, modeling the potential relationship between log K_{DOC} and DOC composition, the log K_{DOC} values for BDE-47, BDE-99, BDE-153 and BDE-154 in four DOC solutions isolated from anaerobic digestion sludge sampled from laboratory and actual biogas plants were first examined to elucidate the high PBDE partition coefficients in the digestate solution by means of an equilibration experiment. Our conclusions can be summarized as follows: The overall log K_{DOC} in our study is higher than the log K_{DOC} in natural water system, researched before. Through the liner regression, we found that the specific category of organic carbon and PBDE molecular structure has a direct impact on the value of log K_{DOC}.

(2) Find out the optimal degradation situation for BDE-209 debromination under both thermophilic and mesophilic condition. BDE-209 from commodity curtain, set as substrate, was first examined to reveal the temperature effect on the anaerobic digestion through a 200 days activity experiment. The generated methane volume during the anaerobic digestion were recorded, and categories of PBDEs as catabolites were analyzed by the GC-EI-QMS. The conclusions can be summarized as follows: through both mesophilic and thermophilic anaerobic digestion, BDE-209 were successfully degraded into less-bromide PBDE products, and non-BDE part in the curtain were decomposed into methane and carbon dioxide. The BDE-209 degradation rate in thermophilic condition is significantly higher than that of mesophilic one, reaching 0.8 $\mu g \cdot day^{-1}$. Furthermore, we found that even under the same cultivation temperatures, the degradation rate increases with the initial BDE-209 dosing mass, and 7.0 is set as the optimal pH of digestate for the digestion. Then the optimal degradation situation for BDE-209 debromination is selected.

(3) Compare the different degradation pathway of BDE-209 anaerobic digestion between thermophilic and mesophilic condition by using chemical reactant BDE-209 as substrate was

examined to clarify the effect of temperature on anaerobic digestion through a 210-day degradation experiment by CSTR and activity experiment in serum bottles at the same time. The conclusions are as follows. With the help of microorganisms, BDE-209 is degraded into nona-, octa- and hepta-BDE by debromination through a multiple-step reaction without any methane generation. Furthermore, owing to the high catalytic activity under the temperature, the rate of BDE-209 degradation under thermophilic conditions is significantly higher than that under mesophilic conditions, reaching a maximum of 1.1 $\mu g \cdot day^{-1}$. Finally, the anaerobic digestion of BDE-209 under both thermophilic and mesophilic conditions fits a first-order reaction kinetics law.

The difference between specific degradation characteristics in thermophilic and mesophilic conditions is examined. And all these findings and the established methodology help us open a wide range of possibilities for the further investigation of PBDE accumulation, transportation, degradation in anaerobic digestion systems of municipal water system.

Future prospective: For the equilibration experiment, DOC would be replaced by the glass beads. Moreover, in this way, the relationship between glass beads diameter and DOC composition, including protein, polysaccharides, lipids concentration, would be investigated. Also, all this thesis focused on the typical PBDE anaerobic degradation. Thus, the no-bromide flame retardants would be the later researching point. The anaerobic degradation of triphenylphosphine, resorcinol-bis(diphenyl phosphate and benzoic acid between thermophilic and mesophilic conditions would also be measured.

References

Ahn, M.Y., Filley, T.R., Jafvert, C.T., Nies, L., Hua, I., Bezares-Cruz, J. 2006. Photodegradation of decabromodiphenyl ether adsorbed onto clay minerals, metal oxides, and sediment. *Environmental Science & Technology*, **40**(1), 215-20.

Akkanen, J., Vogt, R.D., Kukkonen, J.V.K. 2004. Essential characteristics of natural dissolved organic matter affecting the sorption of hydrophobic organic contaminants. *Aquatic Sciences*, **66**(2), 171-177.

An, T., Chen, J., Li, G., Ding, X., Sheng, G., Fu, J., Mai, B., O'Shea, K.E. 2008. Characterization and the photocatalytic activity of TiO_2 immobilized hydrophobic montmorillonite photocatalysts. *Catalysis Today*, **139**(1-2), 69-76.

Arnold, R.G., Teske, S., Tomanek, M., Engstrom, J., Leung, C., Zhang, J., Banihani, Q., Quanrud, D., Ela, W.P., Sáez, A.E. 2008. Fate of Polybrominated Diphenyl Ethers during Wastewater Treatment/Polishing and Sludge Stabilization/Disposal. *Annals of the New York Academy of Sciences*, **1140**(1), 394-411.

Branchi, I., Capone, F., Vitalone, A., Madia, F., Santucci, D., Alleva, E., Costa, L.G. 2005. Early developmental exposure to BDE 99 or Aroclor 1254 affects neurobehavioural profile: interference from the administration route. *Neurotoxicology*, **26**(2), 183-92.

Cai, Z., Jiang, G. 2006. Determination of polybrominated diphenyl ethers in soil from e-waste recycling site. *Talanta*, **70**(1), 88-90.

Cetin, B., Yurdakul, S., Odabasi, M. 2019. Polybrominated diphenyl ethers (PBDEs) pollution in soil of a highly industrialized region (Dilovasi) in Turkey: concentrations, spatial and temporal variations and possible sources. *Environmental Monitoring and Assessment*, **191**(7), 474.

Chen, C.Y., Wang, C.K., Shih, Y.H. 2010. Microbial degradation of 4-monobrominated diphenyl ether in an aerobic sludge and the DGGE analysis of diversity. *Journal of Environmental Science and Health, Part B*, **45**(5), 379-85.

Chen, J., Wang, C., Pan, Y., Farzana, S.S., Tam, N.F. 2018a. Biochar accelerates microbial reductive debromination of 2,2',4,4'-tetrabromodiphenyl ether (BDE-47) in anaerobic mangrove sediments. *Journal of Hazardous Material*, **341**, 177-186.

Chen, J., Zhou, H.C., Wang, C., Zhu, C.Q., Tam, N.F. 2015. Short-term enhancement effect of nitrogen addition on microbial degradation and plant uptake of polybrominated diphenyl ethers (PBDEs) in contaminated mangrove soil. *Journal of Hazardous*

Material, **300**, 84-92.

Chen, M.W., Castillo, B.A.A., Lin, D.Y., Chao, H.R., Tayo, L.L., Gou, Y.Y., Chen, F.A., Huang, K.L. 2018b. Levels of PCDD/Fs, PBDEs, and PBDD/Fs in Breast Milk from Southern Taiwan. *Bulletin of Environmental Contamination and Toxicology*, **100**(3), 369-375.

Chen, Q., Yu, L., Yang, L., Zhou, B. 2012. Bioconcentration and metabolism of decabromodiphenyl ether (BDE-209) result in thyroid endocrine disruption in zebrafish larvae. *Aquatic Toxicology*, **110-111**, 141-8.

Chin, Y.P., Aiken, G.R., Danielsen, K.M. 1997. Binding of pyrene to aquatic and commercial humic substances: The role of molecular weight and aromaticity. *Environmental Science & Technology*, **31**(6), 1630-1635.

Chiou, C.T., McGroddy, S.E., Kile, D.E. 1998. Partition characteristics of polycyclic aromatic hydrocarbons on soils and sediments. *Environmental Science & Technology*, **32**(2), 264-269.

Cho, H.H., Park, J.W., Liu, C.C. 2002. Effect of molecular structures on the solubility enhancement of hydrophobic organic compounds by environmental amphiphiles. *Environmental Toxicology and Chemistry*, **21**(5), 999-1003.

Darnerud, P.O., Aune, M., Larsson, L., Hallgren, S. 2007. Plasma PBDE and thyroxine levels in rats exposed to Bromkal or BDE-47. *Chemosphere*, **67**(9), S386-92.

Deng, D., Guo, J., Sun, G., Chen, X., Qiu, M., Xu, M. 2011. Aerobic debromination of deca-BDE: Isolation and characterization of an indigenous isolate from a PBDE contaminated sediment. *International Biodeterioration & Biodegradation*, **65**(3), 465-469.

Deng, D., Tam, N.F.Y. 2016. Adsorption-uptake-metabolism kinetic model on the removal of BDE-47 by a Chlorella isolate. *Environmental Pollution*, **212**, 290-298.

DePaolis, F., Kukkonen, J. 1997. Binding of organic pollutants to humic and fulvic acids: Influence of pH and the structure of humic material. *Chemosphere*, **34**(8), 1693-1704.

Dietz, R., Gustavson, K., Sonne, C., Desforges, J.P., Riget, F.F., Pavlova, V., McKinney, M.A., Letcher, R.J. 2015. Physiologically-based pharmacokinetic modelling of immune, reproductive and carcinogenic effects from contaminant exposure in polar bears (Ursus maritimus) across the Arctic. *Environmental Research*, **140**, 45-55.

Dunnick, J.K., Pandiri, A.R., Merrick, B.A., Kissling, G.E., Cunny, H., Mutlu, E., Waidyanatha, S., Sills, R., Hong, H.L., Ton, T.V., Maynor, T., Recio, L., Phillips, S.L., Devito, M.J., Brix, A. 2018. Carcinogenic activity of pentabrominated diphenyl ether mixture (DE-71) in rats and mice. *Toxicology Reports*, **5**, 615-624.

Durjava, M.K., ter Laak, T.L., Hermens, J.L., Struijs, J. 2007. Distribution of PAHs and PCBs to dissolved organic matter: high distribution coefficients with consequences for environmental fate modeling. *Chemosphere*, **67**(5), 990-7.

Eriksson, J., Green, N., Marsh, G., Bergman, A. 2004. Photochemical decomposition of 15 polybrominated diphenyl ether congeners in methanol/water. *Environmental Science & Technology*, **38**(11), 3119-25.

Eriksson, P., Jakobsson, E., Fredriksson, A. 2001. Brominated flame retardants: A novel class of developmental neurotoxicants in our environment? *Environmental Health Perspectives*, **109**(9), 903-908.

Eriksson, P., Viberg, H., Jakobsson, E., Orn, U., Fredriksson, A. 2002. A brominated flame retardant, 2,2 ',4,4 ',5-pentabromodiphenyl ether: Uptake, retention, and induction of neurobehavioral alterations in mice during a critical phase of neonatal brain development. *Toxicological Sciences*, **67**(1), 98-103.

Fang, J., Nyberg, E., Winnberg, U., Bignert, A., Bergman, A. 2015. Spatial and temporal trends of the Stockholm Convention POPs in mothers' milk -- a global review. *Environmental Science and Pollution Research*, **22**(12), 8989-9041.

Fang, L., Huang, J., Yu, G., Wang, L. 2008. Photochemical degradation of six polybrominated diphenyl ether congeners under ultraviolet irradiation in hexane. *Chemosphere*, **71**(2), 258-67.

Fang, Z., Qiu, X., Chen, J., Qiu, X. 2011a. Debromination of polybrominated diphenyl ethers by Ni/Fe bimetallic nanoparticles: influencing factors, kinetics, and mechanism. *Journal of Hazardous Materials*, **185**(2-3), 958-69.

Fang, Z., Qiu, X., Chen, J., Qiu, X. 2011b. Degradation of the polybrominated diphenyl ethers by nanoscale zero-valent metallic particles prepared from steel pickling waste liquor. *Desalination*, **267**(1), 34-41.

Farrell, M., Jones, D.L. 2009. Critical evaluation of municipal solid waste composting and potential compost markets. *Bioresource Technology*, **100**(19), 4301-10.

Gerecke, A.C., Giger, W., Hartmann, P.C., Heeb, N.V., Kohler, H.P., Schmid, P., Zennegg, M., Kohler, M. 2006. Anaerobic degradation of brominated flame retardants in sewage sludge. *Chemosphere*, **64**(2), 311-7.

Gerecke, A.C., Hartmann, P.C., Heeb, N.V., Kohler, H.P., Giger, W., Schmid, P., Zennegg, M., Kohler, M. 2005. Anaerobic degradation of decabromodiphenyl ether. *Environmental Science & Technology*, **39**(4), 1078-83.

Guerra, P., Kleywegt, S., Payne, M., Svoboda, M.L., Lee, H.B., Reiner, E., Kolic, T., Metcalfe, C., Smyth, S.A. 2015. Occurrence and Fate of Trace Contaminants during Aerobic and Anaerobic Sludge Digestion and Dewatering. *Journal of Environmental Quality*, **44**(4), 1193-200.

Hassanin, A., Breivik, K., Meijer, S.N., Steinnes, E., Thomas, G.O., Jones, K.C. 2004. PBDEs in European background soils: Levels and factors controlling their distribution. *Environmental Science & Technology*, **38**(3), 738-745.

Hu, Y., Kobayashi, T., Qi, W., Oshibe, H., Xu, K.Q. 2018a. Effect of temperature and organic loading rate on siphon-driven self-agitated anaerobic digestion performance for food waste treatment. *Waste Management*, **74**, 150-157.

Hu, Y., Kobayashi, T., Zhen, G., Shi, C., Xu, K.Q. 2018b. Effects of lipid concentration on thermophilic anaerobic co-digestion of food waste and grease waste in a siphon-driven self-agitated anaerobic reactor. *Biotechnology Reports*, **19**, e00269.

Huang, C., Zeng, Y., Luo, X., Ren, Z., Tang, B., Lu, Q., Gao, S., Wang, S., Mai, B. 2019. In Situ Microbial Degradation of PBDEs in Sediments from an E-Waste Site as Revealed by Positive Matrix Factorization and Compound-Specific Stable Carbon Isotope Analysis. *Environmental Science & Technology*.

Huang, H., Zhang, S., Christie, P. 2011. Plant uptake and dissipation of PBDEs in the soils of electronic waste recycling sites. *Environmental Pollution*, **159**(1), 238-243.

Idris, S.S., Abd Rahman, N., Ismail, K., Alias, A.B., Abd Rashid, Z., Aris, M.J. 2010. Investigation on thermochemical behaviour of low rank Malaysian coal, oil palm biomass and their blends during pyrolysis via thermogravimetric analysis (TGA). *Bioresource Technology*, **101**(12), 4584-92.

Katsoyiannis, A., Samara, C. 2006. The fate of dissolved organic carbon (DOC) in the wastewater treatment process and its importance in the removal of wastewater contaminants. *Environmental Science and Pollution Research - International*, **14**(5), 284-292.

Keum, Y.S., Li, Q.X. 2005. Reductive debromination of polybrominated diphenyl ethers by zerovalent iron. *Environmental Science & Technology*, **39**(7), 2280-6.

Kim, Y.-M., Murugesan, K., Chang, Y.-Y., Kim, E.-J., Chang, Y.-S. 2012. Degradation of polybrominated diphenyl ethers by a sequential treatment with nanoscale zero valent iron and aerobic biodegradation. *Journal of Chemical Technology & Biotechnology*, **87**(2), 216-224.

Knoth, W., Mann, W., Meyer, R., Nebhuth, J. 2007. Polybrominated diphenyl ether in sewage sludge in Germany. *Chemosphere*, **67**(9), 1831-7.

Kuivikko, M., Sorsa, K., Kukkonen, J.V., Akkanen, J., Kotiaho, T., Vahatalo, A.V. 2010. Partitioning of tetra- and pentabromo diphenyl ether and benzo[a]pyrene among water and dissolved and particulate organic carbon along a salinity gradient in coastal waters. *Environmental Toxicology and Chemistry*, **29**(11), 2443-9.

Kuramochi, H., Maeda, K., Kawamoto, K. 2007. Physicochemical properties of selected polybrominated diphenyl ethers and extension of the UNIFAC model to brominated aromatic compounds. *Chemosphere*, **67**(9), 1858-65.

La Guardia, M.J., Hale, R.C., Harvey, E. 2006. Detailed polybrominated diphenyl ether (PBDE) congener composition of the widely used penta-, octa-, and deca-PBDE technical flame-retardant. *Environmental Science & Technology*, **40**(20), 6247-6254.

Lee, L.K., He, J. 2010. Reductive debromination of polybrominated diphenyl ethers by anaerobic bacteria from soils and sediments. *pplied and Environmental Microbiology*, **76**(3), 794-802.

Li, Y.L., He, W., Liu, W.X., Kong, X.Z., Yang, B., Yang, C., Xu, F.L. 2015. Influences of binding to dissolved organic matter on hydrophobic organic compounds in a multi-contaminant system: Coefficients, mechanisms and ecological risks. *Environmental Pollution*, **206**, 461-8.

Liang, D.W., Yang, Y.H., Xu, W.W., Peng, S.K., Lu, S.F., Xiang, Y. 2014. Nonionic surfactant greatly enhances the reductive debromination of polybrominated diphenyl ethers by nanoscale zero-valent iron: mechanism and kinetics. *Journal of Hazardous Materials*, **278**, 592-6.

Liu, Y. 2008. New insights into pseudo-second-order kinetic equation for adsorption. *Colloids and Surfaces A: Physicochemical and Engineering Aspects*, **320**(1-3), 275-278.

Liu, Y., Zheng, G.J., Yu, H., Martin, M., Richardson, B.J., Lam, M.H., Lam, P.K. 2005. Polybrominated diphenyl ethers (PBDEs) in sediments and mussel tissues from Hong Kong marine waters. *Marine Pollution Bulletin*, **50**(11), 1173-84.

Luo, J., Chen, Y., Feng, L. 2016. Polycyclic Aromatic Hydrocarbon Affects Acetic Acid Production during Anaerobic Fermentation of Waste Activated Sludge by Altering Activity and Viability of Acetogen. *Environmental Science & Technology*, **50**(13), 6921-9.

Lyu, Y., Xu, T., Li, X., Cheng, T., Yang, X., Sun, X., Chen, J. 2016. Size distribution of particle-

associated polybrominated diphenyl ethers (PBDEs) and their implications for health. *Atmospheric Measurement Techniques*, **9**(3), 1025-1037.

Mata-Alvarez, J., Mace, S., Llabres, P. 2000. Anaerobic digestion of organic solid wastes. An overview of research achievements and perspectives. *Bioresource Technology*, **74**(1), 3-16.

Matsukami, H., Suzuki, G., Someya, M., Uchida, N., Tue, N.M., Tuyen, L.H., Viet, P.H., Takahashi, S., Tanabe, S., Takigami, H. 2017. Concentrations of polybrominated diphenyl ethers and alternative flame retardants in surface soils and river sediments from an electronic waste-processing area in northern Vietnam, 2012-2014. *Chemosphere*, **167**, 291-299.

McGrath, T.J., Ball, A.S., Clarke, B.O. 2017. Critical review of soil contamination by polybrominated diphenyl ethers (PBDEs) and novel brominated flame retardants (NBFRs); concentrations, sources and congener profiles. *Environmental Pollution*, **230**, 741-757.

Miyazawa, M., Pavan, M.A., de Oliveira, E.L., Ionashiro, M., Silva, A.K. 2000. Gravimetric determination of soil organic matter. *Brazilian Archives Of Biology And Technology*, **43**(5), 475-478.

Moon, H.B., Choi, M., Yu, J., Jung, R.H., Choi, H.G. 2012. Contamination and potential sources of polybrominated diphenyl ethers (PBDEs) in water and sediment from the artificial Lake Shihwa, Korea. *Chemosphere*, **88**(7), 837-43.

Moon, H.B., Kannan, K., Choi, M., Yu, J., Choi, H.G., An, Y.R., Choi, S.G., Park, J.Y., Kim, Z.G. 2010. Chlorinated and brominated contaminants including PCBs and PBDEs in minke whales and common dolphins from Korean coastal waters. *Journal of Hazardous Materials*, **179**(1-3), 735-41.

Moon, H.B., Kannan, K., Lee, S.J., Choi, M. 2007. Polybrominated diphenyl ethers (PBDEs) in sediment and bivalves from Korean coastal waters. *Chemosphere*, **66**(2), 243-51.

Moreira Bastos, P., Eriksson, J., Vidarson, J., Bergman, A. 2008. Oxidative transformation of polybrominated diphenyl ether congeners (PBDEs) and of hydroxylated PBDEs (OH-PBDEs). *Environmental Science and Pollution Research*, **15**(7), 606-13.

Parry, E., Zota, A.R., Park, J.S., Woodruff, T.J. 2018. Polybrominated diphenyl ethers (PBDEs) and hydroxylated PBDE metabolites (OH-PBDEs): A six-year temporal trend in Northern California pregnant women. *Chemosphere*, **195**, 777-783.

Patil, S., Sandberg, A., Heckert, E., Self, W., Seal, S. 2007. Protein adsorption and cellular

uptake of cerium oxide nanoparticles as a function of zeta potential. *Biomaterials*, **28**(31), 4600-4607.

Ramu, K., Kajiwara, N., Tanabe, S., Lam, P.K., Jefferson, T.A. 2005. Polybrominated diphenyl ethers (PBDEs) and organochlorines in small cetaceans from Hong Kong waters: levels, profiles and distribution. *Marine Pollution Bulletin*, **51**(8-12), 669-76.

Rice, D.C., Reeve, E.A., Herlihy, A., Zoeller, R.T., Thompson, W.D., Markowski, V.P. 2007. Developmental delays and locomotor activity in the C57BL6/J mouse following neonatal exposure to the fully-brominated PBDE, decabromodiphenyl ether. *Neurotoxicology and Teratology*, **29**(4), 511-20.

Richardson, V.M., Staskal, D.F., Ross, D.G., Diliberto, J.J., DeVito, M.J., Birnbaum, L.S. 2008. Possible mechanisms of thyroid hormone disruption in mice by BDE 47, a major polybrominated diphenyl ether congener. *Toxicology and Applied Pharmacology*, **226**(3), 244-50.

Robrock, K.R., Coelhan, M., Sedlak, D.L., Alvarez-Cohent, L. 2009. Aerobic biotransformation of polybrominated diphenyl ethers (PBDEs) by bacterial isolates. *Environmental Science & Technology*, **43**(15), 5705-11.

Robrock, K.R., Korytar, P., Alvarez-Cohen, L. 2008. Pathways for the anaerobic microbial debromination of polybrominated diphenyl ethers. *Environmental Science & Technology*, **42**(8), 2845-52.

Roscales, J.L., Munoz-Arnanz, J., Ros, M., Vicente, A., Barrios, L., Jimenez, B. 2018. Assessment of POPs in air from Spain using passive sampling from 2008 to 2015. Part I: Spatial and temporal observations of PBDEs. *Science of the Total Environment*, **634**, 1657-1668.

Sanchez-Prado, L., Llompart, M., Lores, M., Garcia-Jares, C., Cela, R. 2005. Investigation of photodegradation products generated after UV-irradiation of five polybrominated diphenyl ethers using photo solid-phase microextraction. *Journal of Chromatography A*, **1071**(1-2), 85-92.

Schreiber, T., Gassmann, K., Gotz, C., Hubenthal, U., Moors, M., Krause, G., Merk, H.F., Nguyen, N.H., Scanlan, T.S., Abel, J., Rose, C.R., Fritsche, E. 2010. Polybrominated diphenyl ethers induce developmental neurotoxicity in a human in vitro model: evidence for endocrine disruption. *Environ Health Perspect*, **118**(4), 572-8.

Shao, L., Wang, T., Li, T., Lu, F., He, P. 2013. Comparison of sludge digestion under aerobic and anaerobic conditions with a focus on the degradation of proteins at mesophilic

temperature. *Bioresource Technology*, **140**, 131-7.

Shi, G., Yin, H., Ye, J., Peng, H., Li, J., Luo, C. 2013. Aerobic biotransformation of decabromodiphenyl ether (PBDE-209) by Pseudomonas aeruginosa. *Chemosphere*, **93**(8), 1487-93.

Shih, Y.H., Tai, Y.T. 2010. Reaction of decabrominated diphenyl ether by zerovalent iron nanoparticles. *Chemosphere*, **78**(10), 1200-6.

Shih, Y.H., Wang, C.K. 2009. Photolytic degradation of polybromodiphenyl ethers under UV-lamp and solar irradiations. *Journal of Hazardous Materials*, **165**(1-3), 34-8.

Shin, M., Duncan, B., Seto, P., Falletta, P., Lee, D.Y. 2010. Dynamics of selected pre-existing polybrominated diphenylethers (PBDEs) in municipal wastewater sludge under anaerobic conditions. *Chemosphere*, **78**(10), 1220-4.

Siebielska, I., Sidelko, R. 2015. Polychlorinated biphenyl concentration changes in sewage sludge and organic municipal waste mixtures during composting and anaerobic digestion. *Chemosphere*, **126**, 88-95.

Smidt, E., Tintner, J., Böhm, K., Binner, E. 2011. Transformation of biogenic waste materials through anaerobic digestion and subsequent composting of the residues–A case study. *Dynamic Soil, Dynamic Plant*, **5**, 63-69.

Soderstrom, G., Sellstrom, U., de Wit, C.A., Tysklind, M. 2004. Photolytic debromination of decabromodiphenyl ether (BDE 209). *Environmental Science & Technology*, **38**(1), 127-32.

Song, M., Luo, C., Li, F., Jiang, L., Wang, Y., Zhang, D., Zhang, G. 2015. Anaerobic degradation of polychlorinated biphenyls (PCBs) and polychlorinated biphenyls ethers (PBDEs), and microbial community dynamics of electronic waste-contaminated soil. *Science of the Total Environment*, **502**, 426-33.

Stasinakis, A.S. 2012. Review on the fate of emerging contaminants during sludge anaerobic digestion. *Bioresource Technology*, **121**, 432-40.

Stenzel, A., Goss, K.U., Endo, S. 2013. Determination of polyparameter linear free energy relationship (pp-LFER) substance descriptors for established and alternative flame retardants. *Environmental Science & Technology*, **47**(3), 1399-406.

Stiborova, H., Vrkoslavova, J., Lovecka, P., Pulkrabova, J., Hradkova, P., Hajslova, J., Demnerova, K. 2015a. Aerobic biodegradation of selected polybrominated diphenyl ethers (PBDEs) in wastewater sewage sludge. *Chemosphere*, **118**, 315-21.

Stiborova, H., Vrkoslavova, J., Pulkrabova, J., Poustka, J., Hajslova, J., Demnerova, K. 2015b.

Dynamics of brominated flame retardants removal in contaminated wastewater sewage sludge under anaerobic conditions. *Science of the Total Environment*, **533**, 439-45.

Suominen, K., Verta, M., Marttinen, S. 2014. Hazardous organic compounds in biogas plant end products--soil burden and risk to food safety. *Science of the Total Environment*, **491-492**, 192-9.

Takahashi, S., Tue, N.M., Takayanagi, C., Tuyen, L.H., Suzuki, G., Matsukami, H., Viet, P.H., Kunisue, T., Tanabe, S. 2016. PCBs, PBDEs and dioxin-related compounds in floor dust from an informal end-of-life vehicle recycling site in northern Vietnam: contamination levels and implications for human exposure. *Journal of Material Cycles and Waste Management*, **19**(4), 1333-1341.

Tang, S., Yin, H., Chen, S., Peng, H., Chang, J., Liu, Z., Dang, Z. 2016. Aerobic degradation of BDE-209 by Enterococcus casseliflavus: Isolation, identification and cell changes during degradation process. *Journal of Hazardous Materials*, **308**, 335-42.

ter Laak, T.L., Van Eijkeren, J.C., Busser, F.J., Van Leeuwen, H.P., Hermens, J.L. 2009. Facilitated transport of polychlorinated biphenyls and polybrominated diphenyl ethers by dissolved organic matter. *Environmental Science & Technology*, **43**(5), 1379-85.

Tiedje, J.M., Quensen, J.F., 3rd, Chee-Sanford, J., Schimel, J.P., Boyd, S.A. 1993. Microbial reductive dechlorination of PCBs. *Biodegradation*, **4**(4), 231-40.

Tokarz, J.A., 3rd, Ahn, M.Y., Leng, J., Filley, T.R., Nies, L. 2008. Reductive debromination of polybrominated diphenyl ethers in anaerobic sediment and a biomimetic system. *Environmental Science & Technology*, **42**(4), 1157-64.

Uhle, M.E., Chin, Y.P., Aiken, G.R., McKnight, D.M. 1999. Binding of polychlorinated biphenyls to aquatic humic substances: The role of substrate and sorbate properties on partitioning. *Environmental Science & Technology*, **33**(16), 2715-2718.

Viberg, H., Fredriksson, A., Eriksson, P. 2007. Changes in spontaneous behaviour and altered response to nicotine in the adult rat, after neonatal exposure to the brominated flame retardant, decabrominated diphenyl ether (PBDE 209). *Neurotoxicology*, **28**(1), 136-42.

Viberg, H., Mundy, W., Eriksson, P. 2008. Neonatal exposure to decabrominated diphenyl ether (PBDE 209) results in changes in BDNF, CaMKII and GAP-43, biochemical substrates of neuronal survival, growth, and synaptogenesis. *Neurotoxicology*, **29**(1), 152-9.

Wang, S., Zhang, S., Huang, H., Niu, Z., Han, W. 2014. Characterization of polybrominated diphenyl ethers (PBDEs) and hydroxylated and methoxylated PBDEs in soils and plants from an e-waste area, China. *Environmental Pollution*, **184**, 405-413.

Wang, T., Li, S., Zhang, C., Li, Y. 2015. Quantities, sources and adsorption of polybrominated diphenyl ethers in components of surficial sediments collected in Songhua River (Jilin City), China. *Chemosphere*, **119**, 1208-1216.

Wang, W., Delgado-Moreno, L., Ye, Q., Gan, J. 2011. Improved measurements of partition coefficients for polybrominated diphenyl ethers. *Environmental Science & Technology*, **45**(4), 1521-7.

Wei-Haas, M.L., Hageman, K.J., Chin, Y.P. 2014. Partitioning of polybrominated diphenyl ethers to dissolved organic matter isolated from Arctic surface waters. *Environmental Science & Technology* **48**(9), 4852-9.

Wei, H., Zou, Y., Li, A., Christensen, E.R., Rockne, K.J. 2013. Photolytic debromination pathway of polybrominated diphenyl ethers in hexane by sunlight. *Environmental Pollution*, **174**, 194-200.

Wei, Y., Li, J., Shi, D., Liu, G., Zhao, Y., Shimaoka, T. 2017. Environmental challenges impeding the composting of biodegradable municipal solid waste: A critical review. *Resources, Conservation and Recycling*, **122**, 51-65.

Xin, J., Liu, X., Liu, W., Zheng, X.L. 2014. Aerobic transformation of BDE-47 by a Pseudomonas putida sp. strain TZ-1 isolated from PBDEs-contaminated sediment. *Bulletin of Environmental Contamination and Toxicology*, **93**(4), 483-8.

Yan, Y.L., Ma, M.S., Liu, X., Ma, W.F., Li, M., Yan, L.J. 2017. Effect of of biochar on anaerobic degradation of pentabromodiphenyl ether (BDE-99) by archaea during natural groundwater recharge with treated municipal wastewater. *International Biodeterioration & Biodegradation*, **124**, 119-127.

Yang, C.-W., Huang, H.-W., Chao, W.-L., Chang, B.-V. 2014. Bacterial communities associated with aerobic degradation of polybrominated diphenyl ethers from river sediments. *Environmental Science and Pollution Research*, **22**(5), 3810-3819.

Yang, C.W., Huang, H.W., Chang, B.V. 2017. Microbial communities associated with anaerobic degradation of polybrominated diphenyl ethers in river sediment. *ournal of Microbiology, Immunology and Infection*, **50**(1), 32-39.

Yen, J.H., Liao, W.C., Chen, W.C., Wang, Y.S. 2009. Interaction of polybrominated diphenyl ethers (PBDEs) with anaerobic mixed bacterial cultures isolated from river sediment. *Journal of Hazardous Materials*, **165**(1-3), 518-24.

Yuan, J.H., Xu, R.K., Zhang, H. 2011. The forms of alkalis in the biochar produced from crop residues at different temperatures. *Bioresource Technology*, **102**(3), 3488-97.

Zhang, M., Lu, J., Xu, Z., He, Y., Zhang, B., Jin, S., Boman, B. 2015. Removing polybrominated diphenyl ethers in pure water using Fe/Pd bimetallic nanoparticles. *Frontiers of Environmental Science & Engineering*, **9**(5), 832-839.

Zhang, N., Zang, G.L., Shi, C., Yu, H.Q., Sheng, G.P. 2016. A novel adsorbent TEMPO-mediated oxidized cellulose nanofibrils modified with PEI: Preparation, characterization, and application for Cu(II) removal. *Bioresource Technology*, **316**, 11-8.

Zhang, S., Xia, X., Xia, N., Wu, S., Gao, F., Zhou, W. 2013. Identification and biodegradation efficiency of a newly isolated 2,2′,4,4′-tetrabromodiphenyl ether (BDE-47) aerobic degrading bacterial strain. *International Biodeterioration & Biodegradation*, **76**, 24-31.

Zhang, W.-H., Wu, Y.-X., Simonnot, M.O. 2012. Soil Contamination due to E-Waste Disposal and Recycling Activities: A Review with Special Focus on China. *Pedosphere*, **22**(4), 434-455.

Zhao, D.M., Qiao, X.L. 2010. Study on the binding of polyborminated diphnyl ethers to dissolved organic matter, Vol. Master defree. Dalian Univerisity of Technology.

Zhu, X., Zhong, Y., Wang, H., Li, D., Deng, Y., Peng, P. 2019. New insights into the anaerobic microbial degradation of decabrominated diphenyl ether (BDE-209) in coastal marine sediments. *Environmental Science & Technology,* **255**(Pt 2), 113151.

Zhuang, Y., Ahn, S., Luthy, R.G. 2010. Debromination of polybrominated diphenyl ethers by nanoscale zerovalent iron: pathways, kinetics, and reactivity. *Environmental Science & Technology*, **44**(21), 8236-42.

Zhuang, Y., Ahn, S., Seyfferth, A.L., Masue-Slowey, Y., Fendorf, S., Luthy, R.G. 2011. Dehalogenation of polybrominated diphenyl ethers and polychlorinated biphenyl by bimetallic, impregnated, and nanoscale zerovalent iron. *Environmental Science & Technology*, **45**(11), 4896-903.

Zota, A.R., Geller, R.J., Romano, L.E., Coleman-Phox, K., Adler, N.E., Parry, E., Wang, M., Park, J.S., Elmi, A.F., Laraia, B.A., Epel, E.S. 2018. Association between persistent endocrine-disrupting chemicals (PBDEs, OH-PBDEs, PCBs, and PFASs) and biomarkers of inflammation and cellular aging during pregnancy and postpartum. *Environment International*, **115**, 9-20.

Publication List during Ph.D.

Published papers:

Shi, C., Hu, Y., Kobayashi, T., Zhang, N., Kuramochi, H., Zhang, Z., Xu, K.Q., 2019. Anaerobic degradation of decabrominated diphenyl ether contaminated in products: Effect of temperature on degradation characteristics. Bioresource technology 283, 28-35.

Shi, C., Hu, Y., Kobayashi, T., Zhang, N., Zhang, Z., Kuramochi, H., Matsukami, H., Zhang, Z., Xu, K.Q., 2019. Distribution characteristics of poly-brominated diphenyl ethers between water and dissolved organic carbon from anaerobic digestate: Effects of digestion conditions. Chemosphere 223, 358-3653.

Hu, Y., **Shi, C.**, Kobayashi, T., Xu, K.Q., An integrated anaerobic system for on-site treatment of wastewater from food waste disposer, Environmental Science and Pollution Research, accepted, 2019.

Hu, Y., Kobayashi, T., Zhen, G., **Shi, C.**, Xu, K.Q., 2018. Effects of lipid concentration on thermophilic anaerobic codigestion of food waste and grease waste in a siphon-driven self-agitated anaerobic reactor. Biotechnology reports 19, e00269.

Han, H.X., **Shi, C.**, Zhang, N., Yuan, L., Sheng, G.P., 2018. Visible-light-enhanced Cr(VI) reduction at Pd-decorated silicon nanowire photocathode in photoelectrocatalytic microbial fuel cell. The Science of the total environment 639, 1512-1519.

Han, H.-X., **Shi, C.**, Yuan, L., Sheng, G.-P., 2017. Enhancement of methyl orange degradation and power generation in a photoelectrocatalytic microbial fuel cell. Applied Energy 204, 382-389.

Papers in preparation:

Shi, C., Hu, Y., Ma, H.Y., Kobayashi, T., Zhang, N., Kuramochi, H., Zhang, Z., Lei, Z.F., Xu, K.Q., et al., Pathways for the anaerobic degradation of deca-brominated diphenyl ethers in continuous stirred tank reactor under different temperature (Under review).

Shi, C., Hu, Y., Ma, H.Y., Kobayashi, T., Zhang, N., Kuramochi, H., Zhang, Z., Lei, Z.F., Xu, K.Q., et al., Temperature effect on the anaerobic degradation of triphenyl phosphate, diphenyl phosphate and benzoic acid (In contribution).

Presentation:

Shi, C., Hu, Y., Kobayashi, T., Kuramochi, H., Zhang, Z., Xu, K.Q., 2019. Effects of Temperature on the Anaerobic Degradation Pathway of the Deca-bromodiphenyl Ether,

International Conference on Alternative Fuels, Energy and Environment (ICAFEE 2019).

Shi, C., Hu, Y., Kobayashi, T., Kuramochi, H., Xu, K.Q., Zhang, Z., 2019, Effects of temperature on the degradation of poly-brominated diphenyl ethers in anaerobic digestion processes, The 39th International Dioxin Conference pp. 3-PS-291

Shi, C., Hu, Y., Kobayashi, T., Kuramochi, H., Zhang, Z., Xu, K.Q., 2018. Effects of temperature on deca-brominated diphenyl ether anaerobic degradation, International Conference on Alternative Fuels, Energy and Environment (ICAFEE 2018): Future and Challenges pp. 064.

Shi, C., Hu, Y., Kobayashi, T., Kuramochi, H., Xu, K.Q., Zhang, Z., 2018, Effects of organic pollutant from anaerobic digestate on solubility of poly-brominated diphenyl ether in aquatic environment, The 17th World Lake Conference pp. P7-1.

Acknowledgment

I would like to sincerely express my gratitude to my supervisor Prof. Zhenya Zhang, who had provided me the chance to study at Tsukuba University and pursue the Philosophy Doctoral degree. During the three years, Prof. Zhang gave me numerous instructions and precious advises at each stage of my Ph.D. study, which would benefit me in my whole life. I wish to thank Prof. Kai-Qin Xu and Prof. Takuro Kobayashi for their careful guidance during my study at the National Institute for Environmental Studies. The academic knowledge they generously taught me made a firm solid for my future career. Special thanks to Prof. Hidetoshi Kuramochi from National Institute for Environmental Studies on the guidance of the poly-bromodiphenyl Ether analysis. I also wish to thank Prof. Zhongfang Lei and Prof. Kazuya Shimizu for their help in academic problems and career planning. The completion of this thesis is under the guidance and supervision of the thesis committee: Prof. Zhenya Zhang, Prof. Zhongfang Lei, Prof. Kazuya Shimizu, Prof. Kai-Qin Xu. I wish to express my thankfulness to your careful correction and valuable suggestions for my thesis.

I am grateful to researchers in National Institute for Environmental Studies who offered me a lot of help in my study; they are Dr. Yong Hu, Dr. Haiyuan Ma. Thanks to the many delights and help from my friends in Tsukuba University, they are Ms. Hui He, Mr. Zitao Guo, Ms. Xue Zhang, Dr. Qili Hu, Dr. Liting Hao, Ms. Qian Wang, Mr. Qingyue Shen, Dr. Yanfei Cheng, Dr. Tian Yuan, Dr. Shuang Sun, Mr. Long Xiao, Dr. Yong Jiang, Dr. Ying Wang Dr. Qun Dou, Dr. Di Wang, Ms. Qun Wang, Mr. Xuezhi Wang, Mr. Xiaoshuai Li, Ms. Junyi Zhu, Mr. Chenzhu Yin, Dr. Ziwen Zhao, Dr. Jie Li, Dr. Xi Yang, Mr. Yujie Fan and so on.

Best appreciation to technical staff at National Institute for Environmental Studies who provided me with technical guidance, they are Ms. Yuko Kawabe, Ms. Mayumi Katsume, Ms. Yuko Yamanaka, Dr. Kohei Ito, Dr. Hidenori Matsukami, Dr. Toshiyuki Motoki and Dr. Zhenyi Zhang. Same appreciation for Prof. Guoping Sheng and Ms. Hexin Han from the University of Science and Technology of China, who provided much help on my experiment measurement and paper publication. Sincerely thanks to Mr. Yan Xing from the Dalian University of Technology on the many times' modification of my publications. Also, thanks to Mr. Reynald Ponte, Mr. Li Ma, and Mr. Hui Shen, who had many conversations that encouraged me a lot.

Special thanks to Dr. Nan Zhang, who was always accompanying me at both encouraging and harsh moments of Ph.D. study. Finally, I would like to sincerely express my appreciation to my parents and my families; it was their support and caring for me that I can persist on the

way of obtaining a Ph.D. degree.